March 2014

Custom Maximum Power Point Tracker

Hector Emmanuel Alberti Arroyo
Worcester Polytechnic Institute

Mohammad Affan Ghani
Worcester Polytechnic Institute

A Major Qualifying Project
Submitted to the faculty
Of
Worcester Polytechnic Institute

In partial fulfillment of the requirements for the
Degree of Bachelor of Science
In Electrical and Computer Engineering

By

Hector E. Alberti

Mohammad A. Ghani

Date: 03/26/2014

Advised by:

Professor Stephen J. Bitar

Professor John A. McNeil

Sponsored by:

The NECAMSID Lab

ABSTRACT

The purpose of this project was to design a custom Maximum Power Point Tracker (MPPT) for an off-grid charging application. The custom MPPT used a DC/DC buck conversion topology controlled by a Pulse-Width-Modulated (PWM) signal. The duty cycle of this PWM signal was determined according to a Maximum Power Point Tracking algorithm set by a microcontroller. The implemented algorithm performed power calculations and allowed the solar panel to operate at its maximum efficiency. The design was mounted on a Printed Circuit Board and further testing showed that the algorithm was successful in determining the Maximum Power Point of the solar panel with an efficiency greater than 90 percent.

ACKNOWLEDGEMENTS

The Custom Maximum Power Point Tracker project served to be a great challenge, providing a real-world scenario. Dealing with a problem in the energy discipline or any engineering discipline per say, requires a solid background and knowledge of the material and many technical aspects, therefore, prompting the need to refer to existing resources.

Although, through its entirety, the MPPT project demanded hours of crucial design and testing, the end product would not have been a success without the help of the resources provided by the New England Center for Analog and Mixed Signal Design Lab in the Atwater Kent building. Through this lab many integral aspects of the design were tested and tweaked around with to meet the project goals. When waiting parts needed for the design, the many electronic components available in the NECAMSID lab and the ECE Shop were used as substitutes to test many parts of the circuit. This proved to be vital. The MPPT project team is also grateful to the advisor and co-advisor of this project, Professor Stephen J. Bitar and Professor John A. McNeil respectively, for their support and technical feedback throughout the duration of the project. The team also thanks the few members of the previous MQP groups that had similar projects, who proved to be great resources and were kind enough to provide us with their expertise in the area.

Table of Contents

Table of Figures

1.0. INTRODUCTION

In today's world energy has become a serious issue. With the world population on the rise, the demand for power over the last decade has grown exponentially. Through this time we have been relying extensively on natural resources such as coal, oil and gas. This has not only reduced the lifespan of these resources but has also greatly affected our global climate. Therefore, it is crucial that we find and comprehensively adapt renewable and sustainable means of energy generation. This paper sets out to deal with one such source, namely, solar energy. It looks into developing a technique to ensure maximum power is obtained from such a renewable source and allows for compatibility with an off-grid charging station project from the previous year.

1.1. Problem Statement

Adapting these renewable ways of energy harvesting may entail some technical complexity, but for these techniques to be deemed as effective alternatives to fossil fuels it is vital that they be used efficiently in order to maximize power extraction. One potential and ubiquitous renewable energy source is the sun. In recent studies of solar energy harvesting, the extraction of maximum power has been one of the most important research topics. The technique used to ensure that maximum power is obtained from photovoltaic systems is known as maximum power point tracking. This technique commonly implemented in PV systems is carefully monitored through a tracking and controlling system.

Photovoltaic cells have a complex relationship between their operating conditions and the maximum power they can output. Mainly because the solar irradiation that hits the photovoltaic cells in a solar panel has a variable character that is dependent on the season and time of the day. A shadow may be cast on the cell that may be foreseen, as in the case of a tall structure near the solar field or unforeseen, as that created by cloud patterns. Also the energy produced by each photovoltaic cell varies with changes in solar irradiation and temperature. From these considerations, the necessity to identify instant by instant that particular point on the V-I characteristic is necessary to ensure the right operating point is found. With so many parameters and variables at play, designing a controller that effectively tracks and ensures operation at the maximum power point becomes a challenge.

1.2. Project Goals

One of the main goals of this project is to promote the use of renewable energy sources and provide motivation to students at WPI to work on similar projects in the future. Given the energy crisis the world

faces today, it is crucial that students spend time and make use of the resources available at their institutions, to strive towards developing energy efficient and climatically sound techniques that can not only benefit power producers throughout the world but also the environment we live in.

The design of our project uses a maximum power point tracking algorithm to ensure that the solar panel is operating at the highest power point. To ensure that this occurs, there is a need to implement an efficient DC/DC buck conversion topology, as the voltage is being stepped down to 12V to charge the battery. The switching devices used in our converter topology are controlled via a microprocessor. This makes it extremely important to minimize switching losses as we strive for higher efficiency.

An important goal of this project is to design the MPPT to be compatible with the off-grid charging station project from last year. It is important that footprints of our design match to the inputs and outputs of the system that it is being designed for. Another vital goal is to provide an educational value feature. Since our custom MPPT design will be incorporated in the off-grid charging station project from last year it will eventually be placed in the pumpkin lounge in Atwater Kent. Here it will be visible to current and prospective students, faculty members and visitors. Therefore when the charging station is used, it would be an extremely interesting prospect to show the user how the phone or laptop is being charged using a renewable energy source. This will not only attract the attention of prospective students through its design features but will also promote environmental awareness amongst the individuals that pass by.

2.0. BACKGROUND RESEARCH

2.1. Solar Energy System Overview

Solar Energy Systems are aimed to help reduce the use of non-renewable sources of energy as well as to reduce the pollution caused by those. Solar energy offers a greener option while reducing utility cost when used appropriately. Figure 1 shows the main parts of a solar energy system.

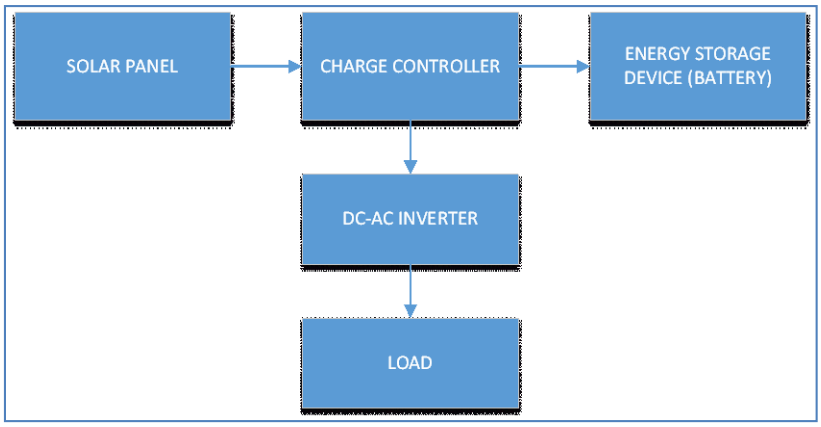

Figure 1. Main Components of a Solar Energy System

Some of the energy radiated by the sun is harvested, and an electrical current is then generated by the solar panel and processed by the charge controller. This provides with a regulated voltage that allows the battery to charge while protecting it from overcharging and discharging. When the battery is fully charged or discharged, the controller disconnects it to prevent from damage.

Then a voltage inverter is used in order to convert the low DC voltage provided by the battery or charge controller to the standard 120VAC that most electronic devices need to operate. Voltage inverters take a low DC voltage (usually 12V to 24V) and use a *DC to DC Boost converter* in order to obtain a higher voltage that can be later modulated using Pulse Width Modulation (PWM) to create a sinusoidal waveform with an RMS voltage of 120V. Other simpler inverters create a square waveform with an RMS voltage of 120V instead of a pure sinusoidal waveform.

In some cases, an inverter is not needed. For instance, if the system is intended to be a USB charger station for phones, a solar-powered calculator, or a charger for a small lithium ion battery of a solar light fixture then a *DC to DC buck converter* is enough to bring the voltage down (or up) to the require voltage and provide it to the device's battery. The only aspect to take into consideration in this case is the maximum power rating for the DC to DC converter and the power that this will have to handle. A more detailed explanation of each component in Figure 1 is presented in the following sections.

2.1.1. Solar Panel

The solar panel (also known as solar cell) is the heart of the system in Figure 1. Its main function is to harvest as much energy as possible and convert it into a flow of electrons (electrical current) that can be then regulated and used by electronic devices. This current can vary depending on the load that is connected to the terminals of the solar panel. When no load is connected, the voltage across the terminals is called the open circuit voltage (V_{OC}). Similarly, when the load has an impedance of zero (short-circuited terminals), the current that flows through the terminals of the panel is called the short-circuit current (I_{SC}). Solar panels range from mini solar cells that can produce less than 1W of power to industrial solar panels that can produce several thousands of watts. It all depends on the applications for which it is intended.

Solar panels have a common characteristic regarding their Voltage-Current relationship. Figure 2 shows the typical Voltage-Current curve of solar cells. As it can be seen, their operation is not linear and there is a tradeoff between voltage and current. Also (something that is not shown) the short circuit current I_{SC} varies as the solar intensity and temperature do. These two values are always specified by the datasheet of the solar panel; however, those are measured under maximum conditions and might represent maximum ratings.

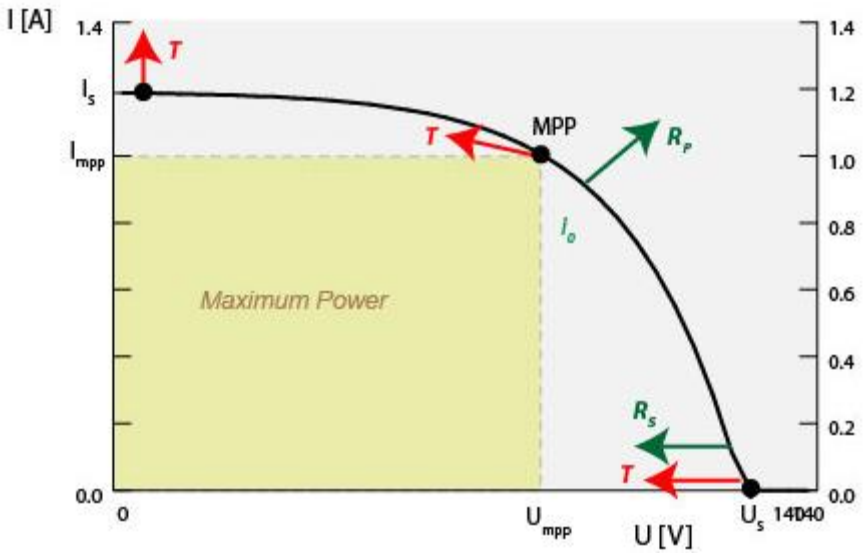

Figure 2. Typical V-I Characteristics of a Solar Panel

The non-linear relationship presented by a solar cell can also be represented by the following equation.

$$I = I_{SC} - I_S\left(e^{\frac{q(V-IR_S)}{AkT}} - 1\right) - \frac{V-IR_S}{R_{SH}} \quad (1)$$

Where V and I are the output voltage and current of the solar panel, I_{SC} is the short circuit current, I_S is the saturation current of the p-n junction (solar panels are basically photodiodes), q is the electron charge, A is the quality factor of the p-n junction, k is the Boltzmann constant, T is the absolute temperature of the solar panel, R_S is the output series resistor and finally R_{SH} is the *shunt* resistance caused by the non-idealities of the p-n junction and presence of impurities near the edges of the cell. This mathematical relationship can also be represented by the electrical circuit in Figure 3.

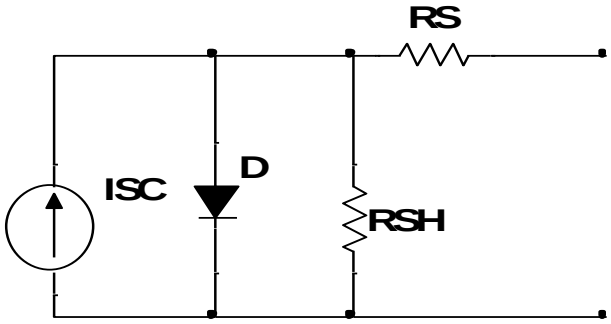

Figure 3. Electrical Model for a Solar Panel

The solar cell equation can be simplified by considering ideal conditions $R_S = 0\Omega$ and $R_{SH} = \infty$. This gives as a result:

$$I = I_{SC} - I_S\left(e^{\frac{qV}{AkT}} - 1\right) \quad (2)$$

Based on Eq. (2), the Open Circuit Voltage (V_{OC}) from Figure 2 corresponds to the case when no current flows through the solar cell and therefore it can be found by making $I = 0A$. This leads to

$$I_{SC} - I_S\left(e^{\frac{qV_{OC}}{AkT}} - 1\right) = 0A$$

And hence,

$$V_{OC} = \frac{AkT}{q}\ln\left(\frac{I_{SC}}{I_S} + 1\right) \quad (3)$$

The previous graphical, mathematical and circuit description of a solar panel show an important fact about the amount of energy that it can provide per unit of time (power). This amount varies depending on the load that is connected at the output of the solar panel; in other words, this power depends on the

operating voltage across the terminals of the solar panel. When a load with a high impedance is connected, the power delivered is approximately zero. Similarly if a load with zero impedance (short-circuit) is connected to it. This brings a big challenge for Electrical Engineers: finding a way of providing appropriate load impedance in order to obtain maximum electrical power from the solar panel.

2.1.2. Charge Controller

Charge controllers aim to provide the correct voltage and current ratings for a rechargeable battery. Some common features should include undercharge and overcharge protection. This is disconnecting the battery from the system when the charge is too low to continue providing energy to the loads. Similarly, the charge controller stops providing energy to the battery when it is fully charged. Failure to do this would clearly lead to a damaged battery.

The key factor of a charge controller is usually DC to DC conversion that allows converting the solar panel voltage to a voltage suitable for charging the battery while protecting it. Implementing a DC to DC converter rather than a linear regulator (or just connecting the battery directly to the solar panel) ensures considerably higher power efficiency.

Some more sophisticated charge controllers possess a smart circuitry that allows not only monitoring the voltage across the solar panel but also changing the load impedance (connected to the panel) so that the solar panel operates at its maximum power. This technology is called Maximum Power Tracking Point (MPPT) and it is discussed in the following section. This is totally possible as depicted in Figure 2.

2.1.3. Battery

The battery is a really important element in the diagram in Figure 1. This element is aimed to store all the energy that is not being used while the solar panel provides it. It acts as an enormous capacitor and therefore, it can provide with enough power when the load requires more power than the amount provided by the solar panel.

Because of its function in the system, the battery has to be rechargeable and its maximum power and current rates have to meet the requirements of the system. These requirements are mainly based on the loads and solar panel. During the charging cycle, if no load is connected to the battery (nor an inverter), then all the power generated by the solar panel is absorbed by the battery. Let P_{in} be the power generated by the solar panel. Then considering an ideal DC to DC converter with no power losses, the power P_{bat} delivered to the battery is equal to P_{in} . Therefore the current flowing through the battery is:

$$I_{bat} = \frac{P_{bat}}{V_{bat}} = \frac{P_{in}}{V_{bat}} \quad (4)$$

Then for a solar panel with a power of 230W (as the one installed in the roof of Atwater Kent building in Worcester Polytechnic Institute) and a common 12V battery, the maximum current through the battery is given by:

$$I_{bat} = \frac{230W}{12V} = 19.17A$$

Therefore the battery maximum current rating has to greater than 19.17A to prevent the battery from damage. This becomes an important factor that should be taken into consideration when evaluating and deciding for the desired battery to use in the system.

2.1.4. DC to AC Inverter

Most electronic devices require an input voltage of 120 VAC or 240 VAC in order to operate under maximum conditions. This poses a problem since normally the voltage across the terminals of a common battery is relatively low DC. Then another device is needed to convert this into the required type and voltage range. This device is called *inverter* and employs DC to AC converters in order to generate a sinusoidal output voltage. Some of the most important parameters of this device are their input voltage range, output voltage range, maximum power ratings, efficiency and output voltage waveform type. Three common output waveforms are the square, square-sinusoidal and pure sinusoidal. These are shown in Figure 4.

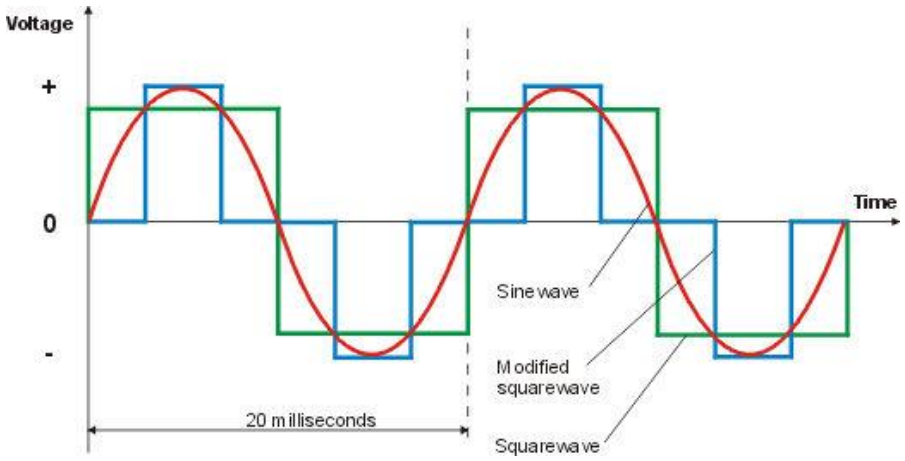

Figure 4- Three Common Output Waveforms from an Inverter

Notice that the sudden changes in the non-pure sinusoidal voltages may generate unwanted transients on the electronic device connected to the inverter. This fact brings an important disadvantage of using these types of inverters. This may damage electronic devices and may shorten their life time.

2.2. Previous Projects

Prior to this project, several projects were conducted in the area of renewable energy and maximum power point tracking. These projects focused on the implementation of renewable energy systems and finding optimum locations for placing renewable energy sources. Each of these previous projects set out to complete one or more of the tasks defined in this project. This project intends to build on the outcomes of some of these projects. Therefore some of these projects analyzed in this section.

2.2.1. Renewable Energy Applications

The original purpose of this project was to design a system that would be featured in the lobby of the Atwater Kent building and would give purpose to the old power panel originally installed in the lounge. After much revision and reconsideration it was concluded that a well-designed power system for the panels was the most feasible option. To aid in the design of such a system contact was made with Jim Dunn, the President of Future Solar LLC. He offered his expertise on the subject matter and donated six solar panels of three different models to the Department of Electrical and Computer Engineering at WPI. Determining an optimal location for these solar panels was crucial for efficient operation. For this purpose Atwater Kent was surveyed using a tool called Solar Pathfinder and the central area of the roof was picked as the best location. Two of the six panels were then installed there.

The focus of this project was to take solar energy from the panels and use it to charge batteries and DC loads such as radios, sensors and computer systems [1]. The completed product was an integrated piece of hardware that used a maximum power point tracking technique and a DC/DC conversion topology on the harvested power, based on a set of user-defined software rules. I2C and RS232 isolated communication ports were also added so that multiple harvesters could communicate with each other via a computer for data collection and analysis.

Although this project underwent many revisions, its essence boils down to what our project sets out to accomplish. Designing circuitry to control the output power of the solar panel by implementing a power point tracking algorithm and controlling the system via a microcontroller are a couple of aspects this “Renewable Energy Applications” project and our “Custom MPPT” have in common. While the project did

promote use of renewable energy applications it directly does not provide sufficient educational value to those who lack thorough knowledge on the subject matter of solar energy operated devices.

2.2.2. Grid Independent Charging Station

One of the main purposes of the "Renewable Energy Applications" project was to encourage project work in the field of sustainability and clean energy and to initiate involvement with the donated solar panels [2]. This purpose was served with the advent of the "Grid-Independent Charging Station" project that resulted in a wall-mounted design of a charging station powered by solar energy.

The purpose of this project was to create a grid-independent charging station. To incorporate a grid-independent power source into the design, one of the two solar panels installed on the roof of Atwater Kent was used. The power coming in from the solar panel was monitored using a Trace 2210RN Solar Charge Controller which implements a maximum power point tracking algorithm and provides a DC/DC conversion topology to charge a 12V lead-acid battery. This 12V battery was then used to provide power to a load to charge laptops and mobile phones via a USB port and an AC outlet. The general power flow of the system is shown below in Figure 4.

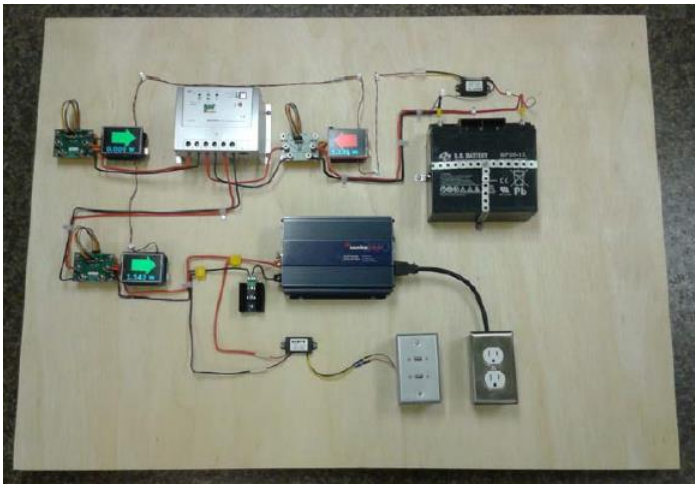

Figure 5- Grid Independent Charging Station Power Flow

The power coming from the solar panel is displayed using a LCD screen controlled by a single-board Arduino Development Board. This power then flows into the charge controller. From the controller, it goes to the 12V battery and to the inverter. In both cases, the power flow is displayed using LCD screens and the Development Board. In the figure above, the solar panel is not connected to the system which is why the power flow to the battery is shown in red, as it serves to be the power source to the system.

This project gives purpose to our design. One of the features of our maximum power point tracker is to be compatible with this system. Also, the educational value that it provided through the power flow display gives motivation to implement an educational purpose to our project. When this wall-mounted power system incorporated with our custom MPPT eventually finds its way into the pumpkin lounge of Atwater Kent, it would be extremely beneficial if it has an interactive design, so the students of the ECE Department are familiar with this environment-friendly system and know the basics behind its operation when they plug in their phones or laptops for charging.

2.3. Market Research

Studying prior art is an integral aspect of a design process. By studying existing designs and products available in the market we were able to get an in-depth understanding of how maximum power point tracker charge controllers function. The project goals and specifications were outlined and some of the existing products in the market were analyzed to see how changing the design can add different features to the charge controller. Below are some of the existing designs for MPPT charge controllers in the market. The project from the "Renewable Energy Applications" MQP was also considered in market research even though the design is not available in the market.

2.3.1. Renewable Energy Applications MQP

Figure 6- Board from Renewable Energy Applications MQP

The "Renewable Energy Applications" project resulted in a complex integrated board which was designed to not only track the maximum power point of the solar panel but also collect and analyze data relating power via its communication ports The board had an extremely flexible design and many features. It served to be a great starting point for our DC/DC conversion topology and talking to one of the team members for the project (Nathaniel Verlee) provided us with some valuable insight regarding potential component and sensor selection. The actual board is shown above in Figure 6.

2.3.2. The Tracer2210RN MPPT Solar Charge Controller

Figure 7- The Tracer 2210RN [3]

The Tracer2210RN MPPT was the charge controller used for the grid-independent charging station project. After a considering a few options the team decided on this component. The Tracer2201RN employs maximum power point tracking and is compatible with 12V systems. The product according to the user's manual, is primarily used in lighting systems, and come with some firmware which employs daylight tracking. This allows the device to be configured to enable output to the load for some time-periods surrounding sunrise and sunset. The Tracer- 2210RN outputs up to 20A, and unit cost was USD 129.00 including shipping on Ebay (B-Term 2012).

2.3.3. The SunSaver MPPT Solar Controller SS-MPPT-15L

Figure 8- The SunSaver MPPT SS-MPPT-15L [4]

The SunSaver charge controller is an advanced maximum power point tracking (MPPT) battery charger for off-grid photovoltaic systems. One of the main features of the controller is that it employs a maximum power point tracking algorithm to maximize the energy harvesting from the PV system. An interesting feature of this product is that it provides load control to prevent over discharge of the battery. This is something that we look to incorporate in our design.

The product is mainly used for 36V or 24V PV arrays to charge either 24V or 12V batteries at 15A. The batteries should be specifically lead acid or nickel cadmium batteries according to the user manual. The system outputs a smaller current compared to the charge controller currently in use for the off-grid system (Tracer2210RN). Operating at a smaller current means that it would be easier to find components to match the current therefore is something we should keep in mind. The controller promises 97.5% peak efficiency, while consuming a current of 35 mA.

2.3.4. MorningStar TS-MPPT Controller-45

Figure 9- The MorningStar MPPT Contoller [5]

The MorningStar TS-MPPT-45 is a versatile charge controller that can be used for 12V, 24V, or 48V solar inputs and can charge a battery between the voltage-range of 8V to 72V at 45A. The manual claims that this controller provides the highest efficiency in the industry. Like most charge controllers this product uses a smart maximum power point tracking algorithm to maximize the energy harvested from the solar array. It effectively and rapidly sweeps the VI characteristic curve to find the maximum operating point. This also enables the product to recognize multiple operating points despite when a cloud passes by resulting in partial shade. This happens only because the curve is swept very fast. The design also includes proprietary tracking to minimize power losses. An additional feature includes an on-board Ethernet for a fully web-enabled interface and includes up to 200 days of data logging. The data logging includes system status which displays V_{MP}, $I_{MP,}$ temperature, and the MPPT shown in Figure 10 below:

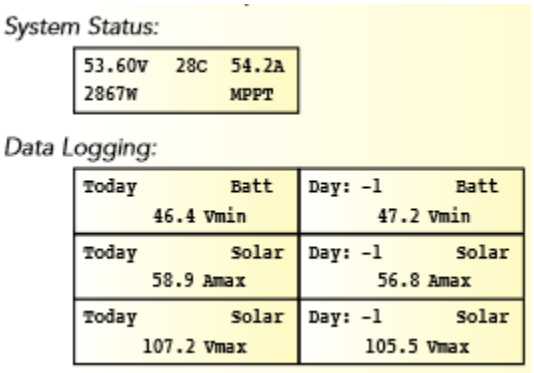

Figure 10- Data-logging Display System

Even though the output current is high for the controller some aspects of this product could be extremely helpful for our design. Firstly, the metering and data logging could be incorporated in a similar way to add educational value to the project design. In order to maximize power harvesting, it is important to minimize power losses.

2.4. Maximum Power Point Tracking

Figure 2 shows the Voltage-Current characteristics of a common solar cell. It can be seen from it that the power delivered by the solar cell depends on the voltage at which this device operates and hence, on the impedance of load connected to it. Figure 11 shows a more detailed illustration of the power delivered by the solar panel as a function of the voltage across its terminals.

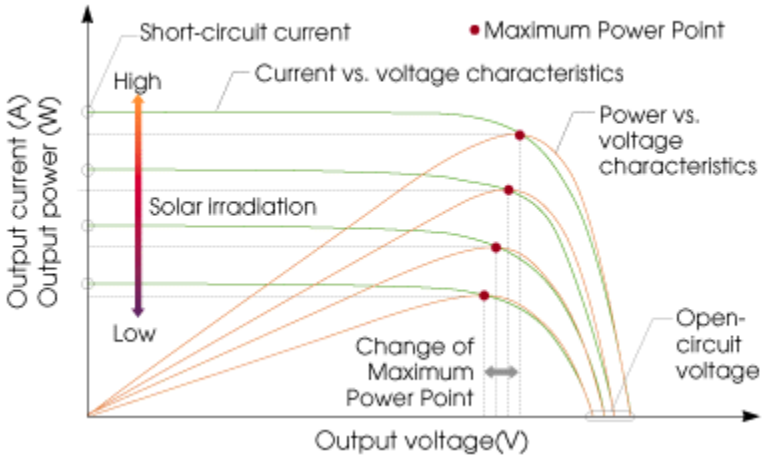

Figure 11- Power-Voltage characteristics of a Solar Cell

Notice that I_{SC} varies with light intensity and temperature and so does the power curve as a function of voltage. The power-voltage curve concaves downwards in the interval from 0V to V_{OC} and has a unique maximum value in that range. This value of voltage is called the Maximum Power Voltage (V_{MP}). The power delivered by the solar cell is given by:

$$P = VI = V\left(I_{SC} - I_S\left(e^{\frac{qV}{AkT}} - 1\right)\right) \tag{5}$$

Then,

$$\frac{dP}{dV} = I_{SC} - I_S\left(e^{\frac{qV}{AkT}} + V\left(\frac{q}{AkT}\right)e^{\frac{qV}{AkT}} - 1\right) \tag{6}$$

Hence the Maximum Power Point Voltage can be found by solving the following equation in the interval from 0 to V_{OC}.

$$I_{SC} - I_S\left(e^{\frac{qV_{MP}}{AkT}} + V\left(\frac{q}{AkT}\right)e^{\frac{qV_{MP}}{AkT}} - 1\right) = 0 \tag{7}$$

However, Eq. (7) can be solved using certain approximation techniques (such as graphical methods or Newton's method) for known values of I_S, I_{SC}, T and A. Notice that Eq. (7) implies that V_{MP} depends on the temperature of the solar cell and the current I_{SC} which in turn depends on light intensity (recall that the other numbers involved are constants). Hence, the challenge for electrical and computers engineers is to design a hardware-software system capable of maximizing the amount of electric energy obtained from the solar cell independently from temperature and light intensity. There is software capable of solving Eq. (7) and a circuitry (hardware) in charge of modifying the load impedance connected to the solar cell so that this can operate at the voltage calculated by the software. This requires constant monitoring of the power delivered by the solar cell and therefore, monitoring the voltage across its terminals and the current that it provides to the system.

2.4.1. MPPT Algorithms

As it was mentioned before, there is the need for not only designing circuitry but coming up with a software approach in order to implement a Maximum Power Point Tracker. This implies the design of an algorithm capable of efficiently and effectively performing the tasks needed for the system. There are several MPPT algorithms than have been designed in order to perform this task and those are presented below [6] [7].

2.4.1.1. Perturb-and-Observe Method (P&O)

This method allows moving the operating point along the curve of the solar panel by modifying the operating voltage accordingly. Its operation is based on calculating the electrical power and then modifying the control loop of the DC to DC converter in order to change the operating voltage and calculating the power delivered by the solar cell again (with this configuration). If the power is higher than

the previous value, then the operating voltage is changed in the same direction as before (if the operating voltage was increased before, then it is increased again; if the operating voltage was decreased before then the operating voltage is decreased). Otherwise, if the power is less than the previous value, the direction of the change is reversed. The change of direction determines the maximum power and therefore the voltage (V_{MP}). This process is repeated over and over while the MPPT is working. This operation is comparable to the linear approximation method used by some Analog to Digital Converters.

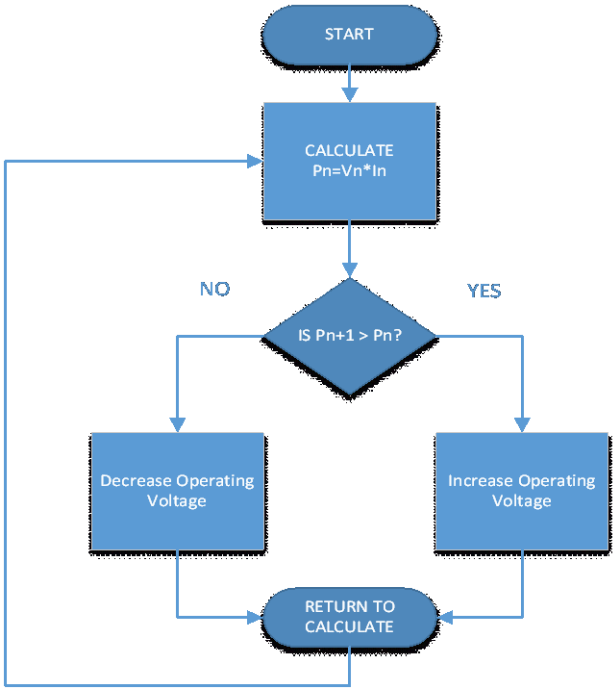

Figure 12- Perturb and Observe Algorithm

The power calculations are performed by measuring the voltage across the terminals of the solar panel and the current that it outputs. The multiplication of both quantities gives the instantaneous power delivered by the solar panel at that moment in time. The operating voltage is changed by modifying the duty cycle of the switching waveform of the DC to DC converter and the power is calculated again.

One of the main advantages that are noticeable in this algorithm is that the operating voltage is always oscillating around the Maximum Power Point. Therefore, large voltage steps would cause relatively high power loses due to these oscillations. Though this problem cannot be eliminated, it can be reduced by having smaller voltage steps. This however, would lead to a slower time response of the system. One way to improve the time response while reducing these oscillations is having a smart voltage step that changes

depending on the point of operation. Larger steps when the system is operating far from the MPP and smaller voltage steps when MPP has been reached.

2.4.1.2. Incremental Conductance Algorithm

This method uses another approximation method in order to find the Maximum Power Point. As pointed by Eq. (8), the Maximum Power Point can be found by differentiating the equation of P with respect to the voltage. This derivative determines the slope of the graph PV; when this slope is positive, the solar panel is operating to the left of the MPP, when it is negative, the solar panel is operating to the right, otherwise the slope is zero and therefore this means that the solar panel is operating at MPP as desired (see Figure 11).

$$\frac{dP}{dV} = \begin{cases} < 0: right\ of\ MPP \\ 0: at\ MPP \\ > 0 Left\ of\ MPP \end{cases}$$

This analysis can be simplified by using the following mathematical approach:

Recall that $P = VI$ and therefore,

$$\frac{dP}{dV} = \frac{d(VI)}{dV} = I\frac{dV}{dV} + V\frac{dI}{dV} \tag{8}$$

Hence,

$$\frac{dP}{dV} = I + V\frac{dI}{dV} \tag{9}$$

At the Maximum Power point, the slope of the Power vs. Voltage curve is zero, when the system operates at the left of this point, the slope of the P-V curve is negative and finally, when the system operates at the right of the MPP, the slope of the curve is positive. This has some implications on Eq. (9) that are shown in Table 1.

Table 1- Incremental Conductance Mathematical Basis

Point of operation	Mathematical characteristics	Approximation
At MPP $\left(\frac{dP}{dV} = 0\right)$	$\frac{dI}{dV} = -\frac{I}{V}$	$\frac{\Delta I}{\Delta V} = -\frac{I}{V}$
Left of MPP $\left(\frac{dP}{dV} < 0\right)$	$\frac{dI}{dV} > -\frac{I}{V}$	$\frac{\Delta I}{\Delta V} > -\frac{I}{V}$
Right of MPP $(\frac{dI}{dV} < -\frac{I}{V})$	$\frac{dI}{dV} < -\frac{I}{V}$	$\frac{\Delta I}{\Delta V} < -\frac{I}{V}$

Recall that $\frac{dI}{dV}$ represents the instantaneous change of I as a function of V and can also be calculated as $\lim_{\Delta V \to 0}(\frac{\Delta I}{\Delta V})$. For small voltage steps, it is common to approximate $\frac{dI}{dV} \approx \frac{\Delta I}{\Delta V}$. The quantity $\frac{\Delta I}{\Delta V}$ is known as incremental conductance while $\frac{I}{V}$ is known as instantaneous conductance, hence the name of the method.

One of the biggest advantages of this method is that the oscillations that the Perturb and Observe method presents are eliminated. This is because this method stops modifying the operating voltage once the Maximum Power Point is reached. If a change of current (outputted by the solar panel) is detected, the system the system starts looking for the new MPP and the process is repeated every time this happens.

2.4.1.3. Current Sweep

The operation of this method is truly based on the graph of the current as a function of the voltage. In fact, this method performs a current sweep in order to obtain the VI characteristics of the solar panel at any moment of time. The MPP is then calculated based on the VI graph obtained. This can be done by varying the duty cycle of the switching waveform from 0% to 100% with a fixed and changing voltage step. In each step, the voltage and current are measured and stored in memory. The smaller the steps are, the more accurate V-I curve is obtained. However, this also increases the time that it takes to generate the curve and hence the time response of the system.

From there it can be concluded that due to the relatively large number of measurements, the time response of this method is highly affected. But considering that the temperature and light conditions do not change fast enough, this could be neglected. However, a more important issue arises with this method: The V-I curve has to be constantly generated every time there is a change in the current outputted by the solar panel. During the V-I curve generation; the solar panel only operates at MPP one time. Therefore, the more voltage steps required to generate the curve, the less power efficiency of the system. However, if the number of steps is too small, the curve might not be generated accurately which leads to erroneous MPP calculations which in turn make the system less efficient.

2.5. DC to DC Converter

A DC to DC converter is an electronic circuit that performs an energy conversion in order to step down, step up a voltage. This type of circuit is widely used in high efficiently power supplies. The main advantage that it has over ordinary linear regulators is that power losses are minimized. Good DC to DC converter designs can achieve an efficiency above 90%. There are three major types of DC to DC converters, *Buck*

converter also known as step down converter, *Boost* converter or step up converter, and *Buck-Boost* converter. The first one converts an input voltage into a lower voltage. For instance a phone car charger uses a buck converter in order to step down from 12V to 5V. The second converter is used to convert a voltage to a higher voltage. And finally, the buck-boost converter can either output a lower or higher voltage depending on the need. Consider for instance that the input voltage varies from 3V to 15V depending on external conditions, but 5V are needed in order to charge a phone, then a buck boost converter can be used. For the purposes of this paper, only the Buck converter is going to be emphasized and explored in the following section.

As mentioned before, a buck converter is used to convert a voltage into a lower voltage. The main idea behind this circuit uses Pulse Width Modulation (PWM) in order to do the power conversion. This technique modulates the width of a square waveform from 0% (fully off) to 100% (fully on). The average voltage of the modulated waveform is a function of its *Duty cycle*. Duty Cycle of a square waveform is defined as the ratio between the time of high state and the period of the waveform. Figure 13 shows a 1 kHz 5V peak square waveform with a 60% duty cycle.

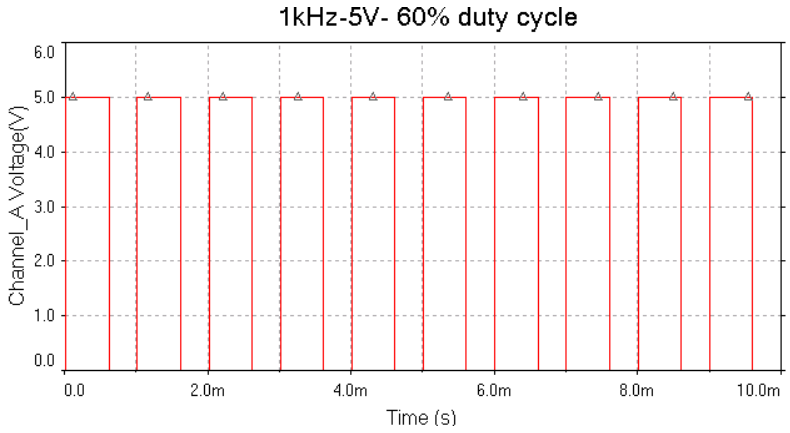

Figure 13- Simulation of a 5V Square Wave (1 kHz Frequency, 60% Duty Cycle)

The principle of the operation is based on the average voltage of the square waveform, this average voltage can be calculated as follows.

$$V_{AVG} = \left(\frac{1}{T}\right)\int_0^T v dt = \left(\frac{1}{T}\right)\int_0^{Ton} V_{in} dt = \frac{T_{on}}{T} V_{in} \quad (10)$$

$$V_{out} = \frac{T_{on}}{T} V_{in} \quad (11)$$

In fact, Eq. (11) describes the relationship of the output voltage of the Buck Converter in Figure 14 [8]. Notice that in the circuit, the input voltage is switched by means of a power transistor Q and the switching waveform Vsw. This allows obtaining a similar waveform as the one in Figure 13.

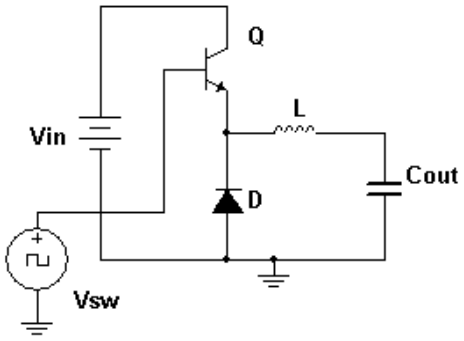

Figure 14-Buck Converter Circuit

The encoded voltage is filtered and the result is the average output voltage. Notice that because the filter is not ideal, there will be ripple voltage across the output capacitor as well as ripple current. The voltage ripple depends on the switching frequency, duty cycle and capacitor C_{OUT}, while the ripple current depends on the switching frequency, the duty cycle, the inductance L and the capacitance of C_{OUT}. Eq. (12) shows the relationship of the ripple output current and the variables mentioned before.

$$\Delta I_{out} = \frac{1}{L} V_{out}(1-D)T_s = \frac{1}{Lf_s} V_{out}(1-D) \quad (12)$$

Where ΔI_{out} is the ripple current, L is the inductance of the output inductor, V_{out} is the aimed output voltage, D is the duty cycle of square waveform that acts as a trigger for the transistor Q and finally T_s is the period of the square waveform.

Another non ideality that has to be taken into consideration when designing a Buck converter is the transients of the circuit. High current and voltage peaks can be generated during the transient. If the peak values of these are higher than the maximum ratings of the components (transistor, Inductor, capacitor, load), then they might result damaged and hence the converter is going to fail and if it does not have an output protection circuit, the load may be also damaged. Figure 15 shows an example of as simulated transient analysis for the current through the output inductor of a Buck converter.

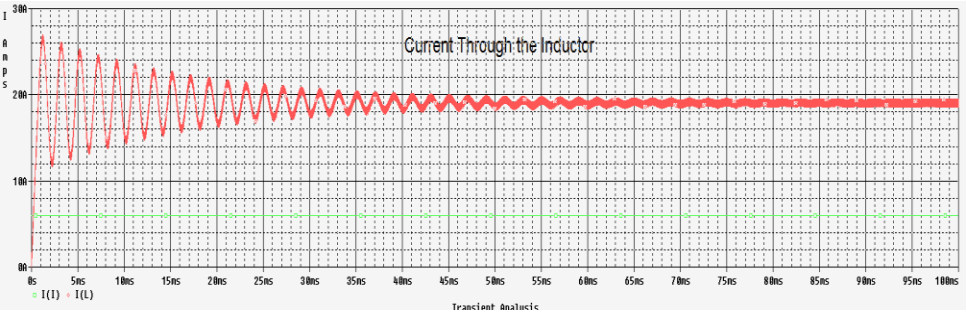

Figure 15-Transient of the Current through the Inductor of a Buck Converter

One way to prevent the transient from having high voltage and current peaks is to slowly increase the duty cycle until it reaches the desired value instead of having the duty cycle fixed. In fact, the duty cycle of a buck converter has to be changing depending on the input voltage. Ideally the input voltage remains constant however, in reality, the input voltage could have a wide range of values and hence, the duty cycle has to change itself in order to obtain constant voltage (or approximately constant) at the output. This is, there has to be a control loop making sure that the output voltage remains in the tolerable bounds. The key factor is monitoring the output voltage and modifying the duty cycle based on these measurements. Monitoring the output current can also help prevent from having high peak currents. If current values higher than certain limit are detected, then the system has to stop increasing the duty cycle until this transient is passed.

The buck converter in Figure 14 is a very efficient device however, there are still power losses. The switching transistor has an internal resistance even when it is operating in "on" state and so do the capacitor, the inductor and the diode. The transistor, capacitor and inductor can be chosen so that their power losses are minimized (cannot be eliminated). There is more control over the diode, and the circuit can be modified so that the efficiency of the system improves. One way to do that is by choosing diodes with low voltage drop across their terminals. Recall that the power dissipated on the diode is $P = V_D I_D$, for the circuit, $I_D = I_{out}$ and hence the only way to reduce that power loss is by making V_D as low as possible. This suggests the use of Shockley diodes. Another approach is to replace the diode with another switching transistor or simply connecting the new transistor in parallel to the diode [9]. The diode in this case, acts as a backup device in case that both transistors overlap turn on at the same time (due to overlapping clocks). The signal used to drive this second transistor has to be the complement of the square waveform that drives the main switching transistor. Both transistors turn on and off alternately without overlapping.

3.0. PROPOSED SYSTEM DESIGN

This chapter discusses the design of the Custom Maximum Power Point Tracker on a system level. For a design to have a solid basis, it is crucial to have a thorough understanding of it on a system level and it is vital to know how different aspects of the design are intertwined and dependent on each other. This chapter sets out to provide and establish these dependencies by highlighting the system components and briefly describing the significant role they play as part of the system, without diving too much into the details of the individual component design.

3.1. Features

The features of the custom Maximum Power Point Tracker were determined directly by analyzing the product requirements. They revolve around the role the MPPT plays in the overall system. One of the most important features of the Maximum Power Point Tracker is to successfully step down the voltage from the solar panel and charge the 12V battery in the system, therefore there is a need to implement an effective DC/DC conversion topology that can accomplish this. The DC/DC conversion application in the system prompts the need for a control loop that uses a microcontroller to ensure that the solar panel operates at the maximum power point. This can be done by controlling the switch in the converter using the Pulse-Width Modulation technique which uses an output pulse from the microcontroller. Figure 16 below shows the characteristic current versus voltage and power versus voltage curves of a solar panel and indicates where this maximum power point occurs:

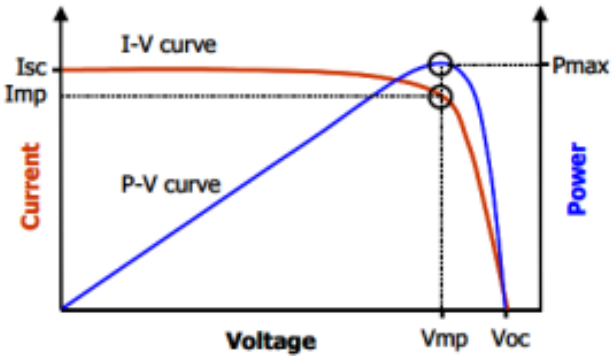

Figure 16. Solar Panel Characteristics

Therefore, by directly modifying the duty cycle of the pulse, the operating point of the solar panel is changed. Another feature that is crucial to any design is protective circuitry. This promotes safety and prevents component damage during unexpected transients of high voltages or currents. Since the MPPT charges a 12V battery, this problem potentially exists. Overcharging and undercharging the battery can

greatly affect its performance, cause unnecessary generation of heat and reduce its life. This is why adding a protective feature to the overall system becomes vital. This feature in the MPPT incorporates overcharging and undercharging prevention techniques that not only isolates the load when the battery is undercharged, so that no more current is drawn from it but also causes the system to readjust the duty cycle of the pulse from the microcontroller when the battery is completely charged. Both of these techniques are dependent on a control system that is monitored and implemented through the microcontroller.

3.2. Block Diagram

An important part of any project is to identify the main components that influence its design. A simple yet effective way to this, is creating a visual that lists the different aspects of design and interconnects them based on the actual configuration in design. Similarly for this project, this was done by creating a system block diagram which can be seen below in Figure 17:

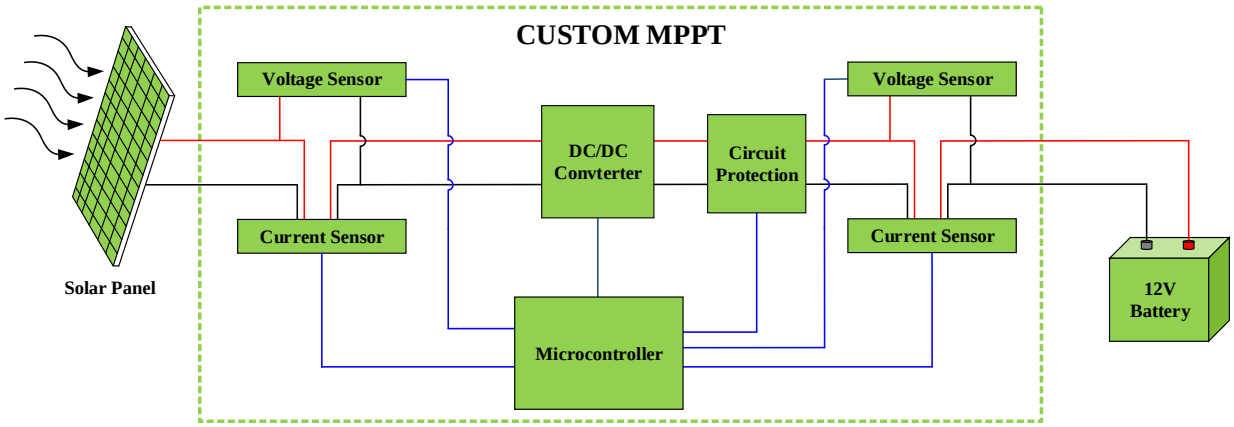

Figure 17. System Block Diagram

The block diagram shown above is a summation of the Maximum Power Point Tracker design on a system level. It highlights the most important features of the design, displays the various connections of the different components shown and specifies where in the system these components can be found. It is evident from the diagram that the system is using solar energy from the solar panel, implementing an effective DC/DC conversion topology that is monitored by a microcontroller and is stepping down the voltage to charge a 12V battery. Also, the additional features like protective circuitry and the sensing blocks are shown. Therefore, the block diagram effectively simplifies the design without diving too much into complicated detail.

3.3. Electrical Requirements

For any given electrical circuit design, one of the most fundamental requirements is a power source. The circuit needs to be complete in order for electrons to flow from and return to the power supply. In most electrical engineering applications, a power supply is used to transfer electrical energy to a load. There are various ways power supplies obtain energy, some of which include:

- Electrical energy transmission systems.
- Storage devices, e.g. batteries and fuel cells.
- Electromechanical systems such as generators and alternators.
- Solar power.

The design of the Maximum Power Point Tracker incorporates two interdependent power sources. One of these power sources is a solar panel that harnesses solar energy from the sun, and is the main driving source of the system. The electrical energy from this power source is stepped down through a DC/DC converter and charges the dependent power source which is a 12V lead acid battery which in turn supplies power to a load. Therefore, ensuring that the electrical requirements of these power sources are met is crucial to design. In essence, these power supplies determines the input and output ratings of the electrical system as the solar panel serves to be the input power supply while the battery serves to be the output power supply. Table 2 below highlights these electrical characteristics:

Table 2. System Properties

	System Electrical Ratings	
	Voltage [V]	**Current [A]**
Input	45	6
Output	12	20

Similarly, as the main system was designed, considering electrical ratings for other components was crucial. This was because fairly complex circuitry was used that suited the application and implemented a DC/DC conversion topology. Working with such circuitry prompts the need of many IC's and electronic components that require constant power to stay on and functional. Therefore, there was a need to outline the electrical characteristics of the different components incorporated in the design to ensure all ratings and specifications were met. The purpose of the MPPT is to charge a 12V battery, after analyzing the existing design it was determined that this voltage source can potentially be utilized and regulated to provide for the electrical needs of some of the IC components used in the system. This proved to be a

significant aspect of the design as the use of an external battery or power source was avoided. Table 3 provides a list of all the components used and their associated power requirements.

Table 3. Component Voltage Ratings

Component Voltage Ratings	
Component	**Voltage [V]**
Microcontroller	5
MOSFET Driver	12
Buffer IC	10
Current Sensors	5
Regulator (12 to 5)	12
Regulator (12 to 10)	12

The components listed above in the table nominally require a minuscule amount of current for operation therefore; the only values listed are the voltage values needed to power these components. The first component serves to be a major part of the system and is the microcontroller which needs an input of 5V to function. Since there was no 5V source in the design, a voltage regular was used to convert the 12V from the battery to 5V for the microcontroller. The next couple of components listed above are the MOSFET Driver (IR2117) and the Buffer IC (TC427). These chips are integrated in the driver circuit which is another crucial part of the design. Both of these chips required supply voltages of 12V and 10V respectively. The IR2117 was supplied with 12V directly from the battery while for the TC427, a second voltage regulator was used to step down the 12V from the battery to 10V to power the chip. Also integrated in the design are current sensors. These current sensors used the same supply voltage as the microprocessor therefore, required the use of the same voltage regulator.

3.4. Buck Converter Design

The normal operation of the conventional buck converter presented in the previous section applies for a relatively fixed input voltage (some fluctuations may be present but the duty cycle compensates in order to get a fixed output voltage) and a changing output voltage that depends both on the input voltage and duty cycle of the switching waveform. This is, given an input voltage, the duty cycle determines the output voltage.

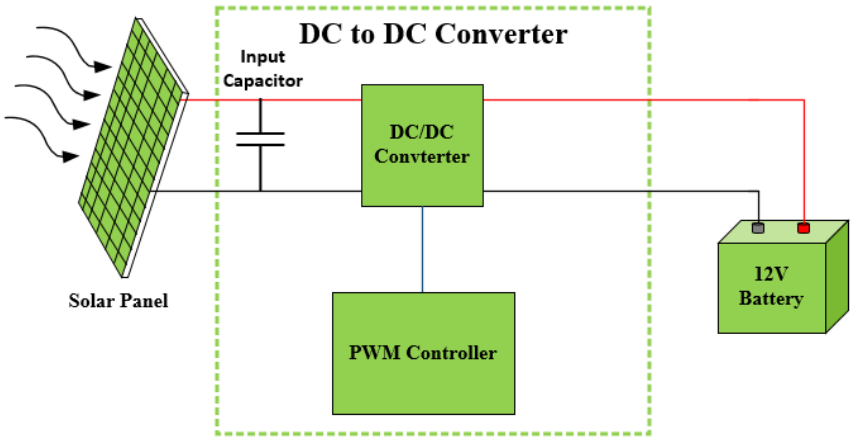

Figure 18. DC to DC Proposed Diagram

A similar approach is used in this project however, for this case it is required to have full control over the input voltage while the output voltage is fixed no matters what the duty cycle of the switching frequency is. This is because a battery is connected to the output of the buck converter and hence, the output voltage will always be equal to the voltage across the battery which is approximately constant (it varies depending on the state of the battery: a fully charged battery will present a higher voltage across its terminals compared to a non-fully charged battery). Recall from the previous section that the voltage across the solar panel depends on impedance of the load connected to it and then due to the power conversion performed by the buck converter, as the duty cycle varies, so does the voltage across the solar panel. This suggest that the load impedance that the solar panel "sees" depends on the duty cycle of the buck converter and therefore the power delivered by the solar panel can be tracked using this technique (modifying the duty cycle). The two extreme cases are when the duty cycle is cero, this is equivalent to have the solar panel connected to an open circuit and therefore it operates at its open circuit voltage and zero current. Similarly when the duty cycle is 100%, the solar panel sees it as a short circuit from its positive voltage terminal to the battery and hence the solar panel operates at 12V and its correspondent current on its V-I curve. Then varying the duty cycle from 0% to 100% makes the solar panel work from its open circuit voltage to the voltage across the battery (approximately 12V).

3.5. Microcontroller

For simplicity, the project implements the Atmega328p-pu and for prototyping, the circuit is initially tested using the Arduino UNO development board. The microcontroller has the functions of reading the data from the sensors, manipulate that data and converting it into the corresponding voltage (in the case of the voltage sensor) or current in the case of the current sensor. With this, both input and output power

can be calculated and the algorithm (also implemented with the microcontroller) tracks the maximum power point.

3.6. Sensors

There are two types of sensors incorporated in the design of the Maximum Power Point Tracker. These include the voltage and current sensors. Since the power point tracking technique actually makes use of a software algorithm that constantly requires readings of the voltage and current values in real-time to run power calculations and monitor system parameters via the microcontroller , it needs the voltage and current values from these sensors. Also, since the design has a protective feature, high current or voltage values can prove detrimental to the components in the design, therefore these values are constantly monitored by the microcontroller through these sensors. This is the reason why two voltage sensors and two current sensors are used; one of each on the input and output side of the system.

Therefore, it is evident that without the sensors, the MPPT system cannot serve its purpose. A more detailed discussion about these sensors is provided in the Detailed Design of the system which is the next chapter. As mentioned earlier, this chapter overviews the design of the Custom MPPT on a system level, so intricate detail of the individual components which in this case are the current and voltage sensors, is avoided.

3.7. Protection Circuitry

The energy delivered by the solar panel is stored in a Lead-Acid battery. This type of batteries have a big capacitance and its cost is relatively low compared to lithium Ion batteries with the same capacity. However, as many other batteries, it is necessary to be careful with the charging algorithm since overcharged or undercharged lead acid batteries represent a high risk of damage of the battery and consequently a fire.

The design includes both overcharge and undercharge protections and a smart algorithm to charge the battery without the risk of damaging it. The protection circuitry is based on a voltage sensor that monitors the voltage across the terminals of the battery and determines the state of the battery (either fully charged, discharged or in between both states).

4.0. DETAILED DESIGN

This chapter discusses the design of the Custom Maximum Power Point Tracker under a more detailed light. While the prior chapter highlighted the major parts of the system and examined them at a system level, this chapter sets out to provide greater depth and a thorough analysis of each component with the aid of graphs, test circuits and technical discussion.

4.1. Buck Converter

The previous section described the proposed buck converter operation qualitatively. This section is aimed to explain and the detail about the design and derive formulas that determine the main components of the design that meet the required specifications. The two main electrical specifications relevant for the design of the buck converter are the maximum power that the buck converter (250W of continuous power) can handle as well as the type of battery to be used as the storage device (12V lead acid battery). The general schematic diagram for this circuit is shown in Figure 19.

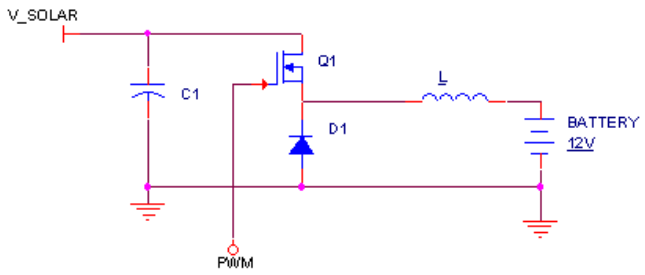

Figure 19. Simplified Asynchronous Buck Converter

In the circuit, the voltage at the output of the buck converter is held approximately constant and equal to the battery voltage while the input voltage varies from the open circuit voltage of the solar panel (when the switch transistor is always off, duty cycle equal 0%) to the battery voltage (when the switch is always off, duty cycle equal to 100%). This leads to the thought that the input voltage contains some ripple that depends on the input capacitor and the duty cycle at which the buck converter operates. Similarly, assuming the battery is an ideal source, the voltage at the output remains constant but the output current contains some ripple that depends on the inductor L and switching frequency.

4.1.1. Inductor

Considering the case of a 100% efficiency buck converter, the current across the inductor (without considering the transient behavior) is given by,

$$I_L = \frac{230W}{12V} = 19.2A$$

This is aimed to be a very robust design therefore the current requirement for the inductor is ideally 30A in order to have a margin of error. As important as the handling current it is the inductance since this determines the amplitude of the ripple current at the output and hence the ripple current that charges the battery. The ripple current has a negative impact on the life of lead acid batteries [10] and therefore the inductor is selected so that the amplitude of the ripple current is as small as possible.

Eq. (12) suggests maximizing the product Lf_s and hence choosin

g a relatively large value for the inductance Hand a high switching frequency. However, there is an important tradeoff between inductance, cost and power consumption, the larger the inductance, the more spires it needs which implies longer wires and hence a larger resistance (due to non-idealities of the wires) and a higher cost. Increasing the inductor size also has an impact on the transient behavior of the buck converter. The time that it takes for the output voltage to stabilize to the steady state is longer as the inductance is larger and hence the time response of the system would get affected.

Considering that the solar conditions do not change too fast, the system does not need to be fast in the order of micro seconds, the inductor was chosen based on the maximum frequency at which the system is able to operate (due to the 16Mhz clock signal used by the microcontroller), the maximum ripple current at the output of the circuit and availability on the market. Cost, size and resistance were also considered but as primarily factors. Using Eq. (12) and considering $f_s = 160kHz$, $V_{out} = 12V$ and D=0 (maximum ripple current), the inductance L would be given by:

$$L = \frac{1}{\Delta I f_s} V_{out}(1 - D) = \frac{75E^{-6}}{\Delta I} \quad [H] \tag{13}$$

That result implies that in order to have a ripple current with a peak to peak amplitude of less than 100mA, the inductance L has to be in the order of mH which represents a relatively large value considering that it current rating of it has to have. For this circuit, it was found an inductor with a nominal inductance of 450uH, a current rating of 36A with convection cooling and 53A with forced air at 3m/s and 1.5mΩ nominal resistance at room temperature [11]. With those electrical characteristics, the estimated ripple current can be calculated as:

$$\Delta I = \frac{1}{Lf_s} V_{out}(1 - D) = \frac{75E^{-6}}{L} = \frac{75E^{-6}}{450E^{-6}} \approx 167mA$$

Also, according to the datasheet of this device, the parasitic resistance due to the relatively long wire that compounds this inductor is 1.5mΩ [11]. Considering the worst case, the maximum power dissipated by the inductor would be given by:

$$P_{IND} = I^2R \leq (19)^2(0.0015) = 0.5415W$$

That represents a considerably small power loss compared to the power dissipated by the MOSFET and the diode. Also, this only represents the 0.23% of the total power considering the maximum power of the solar panel.

4.1.2. Input Capacitor

The circuit shown in Figure 19, the capacitor C1 is connected there to increase efficiency and at the same time stabilize the voltage across the terminals of the solar panel. Without the capacitor, the solar panel would only provide power to the system during the high side of the PWM. This capacitor charges during the low side of the PWM, storing energy that is then discharged during the high side period. Notice that the capacitor charges when the switching transistor is an open circuit and discharges when the transistor is on the conduction state.

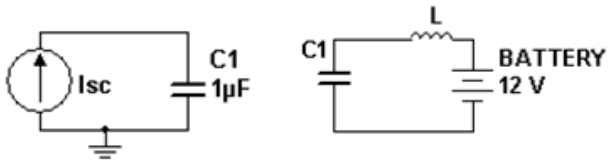

Figure 20. Charging and discharging circuitry for input capacitor

Assuming that the input voltage has reached a steady state, the ripple voltage can be calculated as the maximum value that the capacitor voltage reaches during the low time of the switching waveform (transistor in cutoff). This corresponds to Figure 20 which contains a simplified solar panel model (just as a current source). The voltage at the capacitor can be found as

$$V_{C_1} = V_{C_1}(0) + \frac{1}{C_1}\int_0^{(1-D)T} I_{SOLAR} \quad (14)$$

Assuming $I_{SOLAR} = I_{SC}$, The equation can be simplified as:

$$V_{C_1} = V_{C_1}(0) + \frac{1}{C_1} I_{SC}(1-D)T \quad (15)$$

Hence, the ripple voltage is given by:

$$\Delta V_{C_1} = \frac{1}{C_1} I_{SC}(1-D)T = \frac{1}{C_1 f_s} I_{SC}(1-D) \tag{16}$$

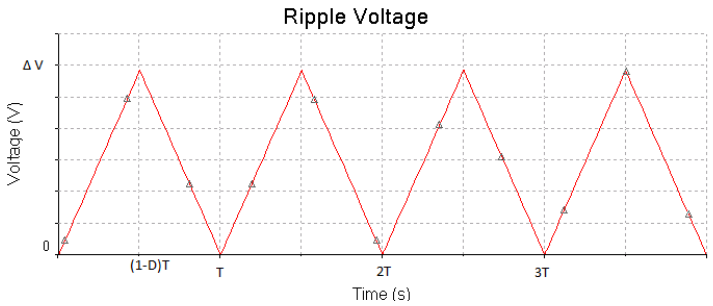

Figure 21. Ripple voltage across the solar panel

Given C_1 and f_s, the ripple voltage at the input of the buck converter depends on the duty cycle only. Since the duty cycle at which the circuit is aimed to operate covers a wide range, it is important to estimate its value that maximizes the ripple voltage. Having a considerably small ripple voltage at the solar panel is vital since the power calculations are based on a voltage divider and a current sensor at that node. Ripple voltage with a considerably high amplitude introduces noise to the power measurements and hence, affect the efficacy of the MPPT algorithm. The amplitude of the ripple voltage has to be smaller than the smallest voltage step caused by a step on the duty cycle of the switching frequency. Assuming that the voltage at the solar panel varies linearly with respect to the duty cycle, the smallest voltage step would be given by:

$$\frac{V_{OC} - V_{BATT}}{Steps} = \frac{48V - 12V}{99} = 364\frac{mV}{Step}$$

Hence,

$$\Delta V_{C_1} = \frac{1}{C_1 f_s} I_{SC}(1-D) < 364\frac{mV}{Step} \tag{17}$$

Again, assuming the worst case scenario with D=0 (according to the equation), $I_{SC} = 6A$ and the switching frequency $f_s = 160kHz$,

$$\frac{(1)}{C_1 f_s} I_{SC} < 364mV \tag{18}$$

$$C_1 > \frac{0.25 I_{SC}}{0.364 f_s} = \frac{6A}{(0.364V)(160000Hz)} \approx 103\mu F$$

Increasing the value of C_1 would reduce the ripple voltage at the input which would make the power calculations more accurate. Then the main filter used for selecting the input capacitor was its capacitance

and of course its rated voltage. C_1 has to be manage to handle approximately 50V and have a low equivalent series resistance ESR. The final value chosen for C_1 was $470\mu F$ and hence the expected maximum ripple voltage is:

$$\Delta V_{C_1} = \frac{6}{0.00047(160000Hz)} = 80mV$$

In case this ripple voltage affects the operation of the MPPT, two of these capacitors will be connected in parallel at the input of the buck converter and the ripple voltage will be halved.

4.1.3. Diode

The selection of the diode is mainly based on the maximum current that could flow through it, power efficiency and maximum breakdown voltage. This diode has to be able to manage the same current as the inductor (19.2A) and hence it was decided to select a diode with a rated current of at least 30A and breakdown voltage of 100V (twice as much as the maximum voltage across the solar panel). For power efficiency purposes, the diode has to feature a low voltage drop across its terminals. This is the reason why it was decided to use a Shockley diode. The actual model of the selected diode is the NTSB30U100CT from ON semiconductors. Its maximum forward current is 30A and its nominal forward voltage 0.42V (with a maximum voltage of 0.8V) [12]. Then, the maximum power dissipated by the diode is given by

$$P_{d\_max} = V_d I_d (1 - D) = (0.8)(19.2)(1 - D) = (1 - D)15.36\ [W] \quad (19)$$

4.1.4. MOSFET switch

First, in order to lower conduction losses, it was decided to use an N-channel MOSFET (their ON resistance is considerably lower compared to a PMOS with the same physical characteristics). Similar to the diode, the NMOS has to handle up to 19.2A reason why the rated current of it has to be at least 30A to have a margin of error. As important as the drain current it is the Drain to Source breakdown voltage. This has to be at greater than the voltage across the solar panel. This is why, it was desired to find a transistor with a breakdown voltage of 100V. Finally, in order to reduce conduction losses, the on resistance has to be as low as possible.

Current rating, breakdown voltage, on resistance and finally cost were the aspects taken into consideration for choosing the right NMOS. The one selected is the STB30NF10 from STMicroelectronis. Its main characteristics are depicted on Table 4 [13].

Table 4. STB30NF10 main characteristics

Symbol	Parameter	Value	Unit
VDS	Drain to source voltage	100	V
VGS	Gate to Source voltage	-20	V
ID	Drain current at 25C	35	A
ID	Drain current at 100C	25	A
RON	ON resistance max	0.045	Ω
T_j	Junction to Case Resistance	-55 to 175	C
R_{jC}	Thermal Resistance junction to case max	1.3	C/W

Using the information in the table and considering the highest current that will possible flow through the MOSET, the power dissipation due to conduction loses is given by:

$$P_Q = (0.045)(19.2^2)(D) = 16.6D\ [W] \tag{20}$$

This implies the need for a heat sink in order to prevent the device from breaking down due to overheating. Assuming the thermal resistance between case and heat sink to be 0 °C/W, the required thermal resistance of the heat sink R_H is given by:

$$R_H = \frac{T_j - P_Q R_{jC} - T_{amb}}{P_Q} \tag{21}$$

Where T_{amb} is the ambient temperature. Assuming $T_j = 100°\text{C}$ and $T_{amb} = 25°\text{C}$,

$$R_H = \frac{75 - 16.6(1.3)}{16.6} = 3.22\ °\text{C/W}$$

In order to make the system more robust, two MOSFET will be used in parallel each of them featuring a $2.7\ °\text{C/W}$ heatsink. This will make sure that the junction temperature remains at a low temperature preventing it to break due to over temperature.

4.1.5. Simulations

Before prototyping the proposed DC to DC converter, the circuit was simulated in order to prove the expected behavior. The simulations take into consideration the on resistance of the MOSFET, the voltage drop across the diode, the internal resistance of the battery, the equivalent series resistance of the capacitor and most non idealities of the components. The main purposes of the simulations are first, to prove that the voltage across the solar panel decreases as the duty cycle of the PWM signal increases (and vice versa). Second, that the amplitude of the ripple voltage present at the input of the buck converter is low enough to implement an effective MPPT algorithm. Third, that the amplitude of the ripple current through the inductor is low enough to prevent the battery from damage. And finally to calculate the power dissipated on the power diode and power MOSFET. All simulations were run on PSPICE due to its great amount of flexibility and tools. Since algorithm cannot be "programmed" onto PSPICE, the behavior was simply analyzed for different values of the duty cycle and the expected parameters are compared to the simulated parameters. Figure 22 below shows the voltage at the input of the buck converter. Notice that it depends on the value of the duty cycle (as expected). Also notice that there is a transient caused by the sudden change of the duty cycle of the PWM (from D=0% to the value of D).

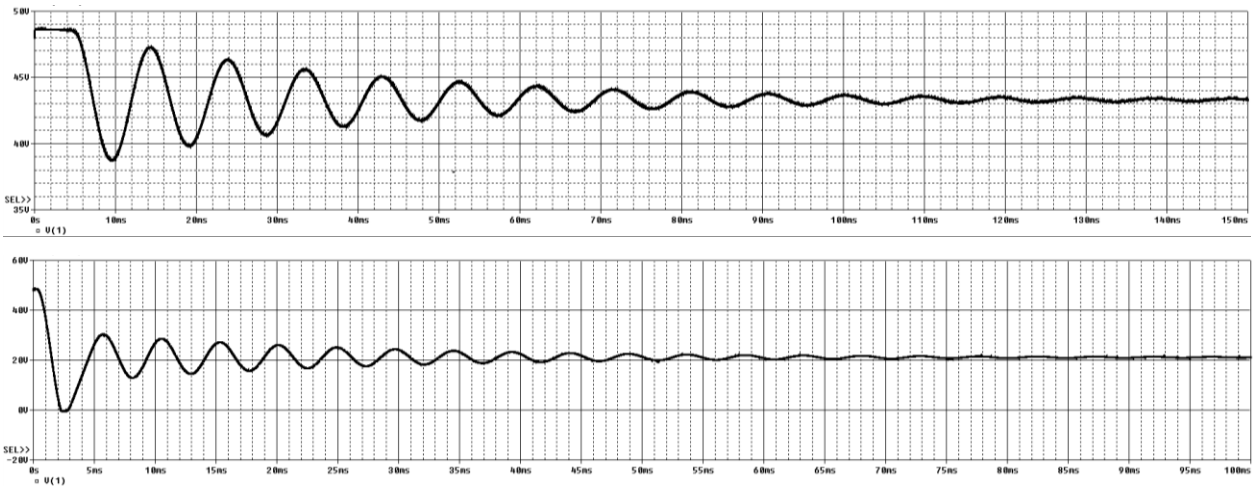

Figure 22. Input Voltage at D=30% (Top) and 60% (Bottom)

Figure 23 and Table 5 contain the voltage at the input when it reaches its steady state with respect to the duty cycle. It is important to mention that the transients caused by the sudden changes in PWM will be diminished by smoothing the variation of the PWM. This is, increasing or decreasing the duty cycle by the smallest possible step. This may represent a slower time response of the system however, it will protect the system from high voltage and current transients that may result on the damage of the components of the system.

Table 5- Input Voltage

Duty Cycle	V_in [V]
10%	48.642
20%	48.642
30%	43.293
40%	32.183
50%	25.536
60%	21.114
70%	17.96
80%	15.597
90%	13.762
99%	12.428

This information can be better analyzed by plotting the voltage across the solar panel vs. the duty cycle at which the DC to DC converter operates at that moment. This graph is shown Figure 23 and a best fitting line has been added in order to model the behavior of the input voltage as a function of the duty cycle which was previously assumed to me linear in de design.

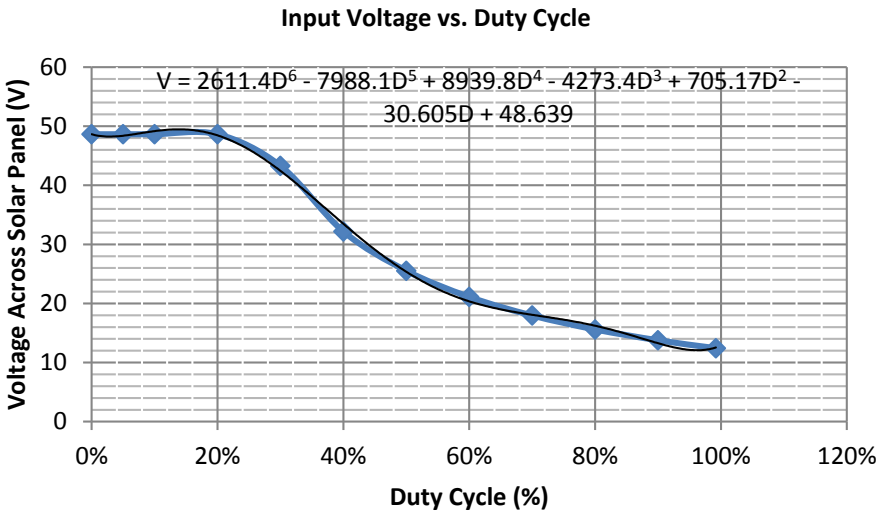

Figure 23. Voltage across the Solar Panel as a Function of Duty Cycle.

The graph above shows that the relationship between the voltage across the solar panel and the duty cycle is far from being linear. Instead, It can be modeled by a sixth degree polynomial with a domain than ranges from D=0 to D=100%. In further studies, it would be extremely important to analyze this correspondence between both parameters and of course, determine if there is a better best fitting line that matches this behavior. It would also be imperative to derive a mathematical formula based on the proposed circuit. This non linearity relationship between the input voltage and the duty cycle also suggest

a non-linearity between the duty cycle and the ripple voltage and current. The values for those parameters obtained with the simulations are shown in Table 6.

Table 6. Current and Voltage Ripples varying with Duty Cycle

Duty Cycle	ΔV_{SOLAR} [mV]	ΔI_{OUT} [mA]
10%	3.00E-05	5.20E-02
20%	1.40E-04	1.00E-01
30%	0.0558	0.13
40%	0.048	0.111
50%	0.0417	0.094
60%	0.032	0.072
70%	0.024	0.0525
80%	1.51E-02	0.0347
90%	8.00E-03	0.0173
99%	6.20E-04	0.0323

Notice that as expected, varying the duty cycle of the PWM, varies the amplitude of both ripple voltage and current; as suggested before, the relationship is not linear (as shown in Figure 24) . However, this is not a relevant detail in the implementation of the MPPT. As long as the amplitude of the ripple voltage is below 364mV.

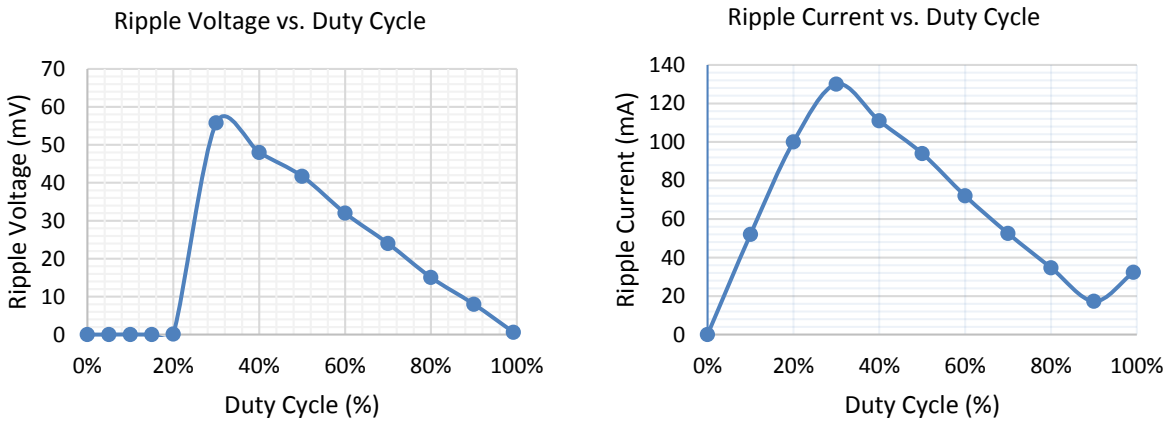

Figure 24. Input Voltage Ripple vs. Duty Cycle (left) and Output Ripple Current vs. Duty Cycle (right)

The simulations show a really small ripple voltage at the input and ripple current at the output. Their maximum values according to the data, are 55.8mV and 130 mA respectively. This small ripple voltage will allow accurately measuring the input voltage and hence effectively performing the MPPT algorithm (with an accurate current sensor). The small ripple current on the output of the DC to DC converter helps safely charging the battery and therefore protecting the lifespan of it.

Nevertheless, power dissipation was also simulated and calculated. This was done in order to verify that the actual power dissipated was below the calculated values shown in the previous subsection. Both power dissipated on the switching device (NMOS) and power diode were averaged over each period and their steady values plotted vs. Duty cycle on Figure 25.

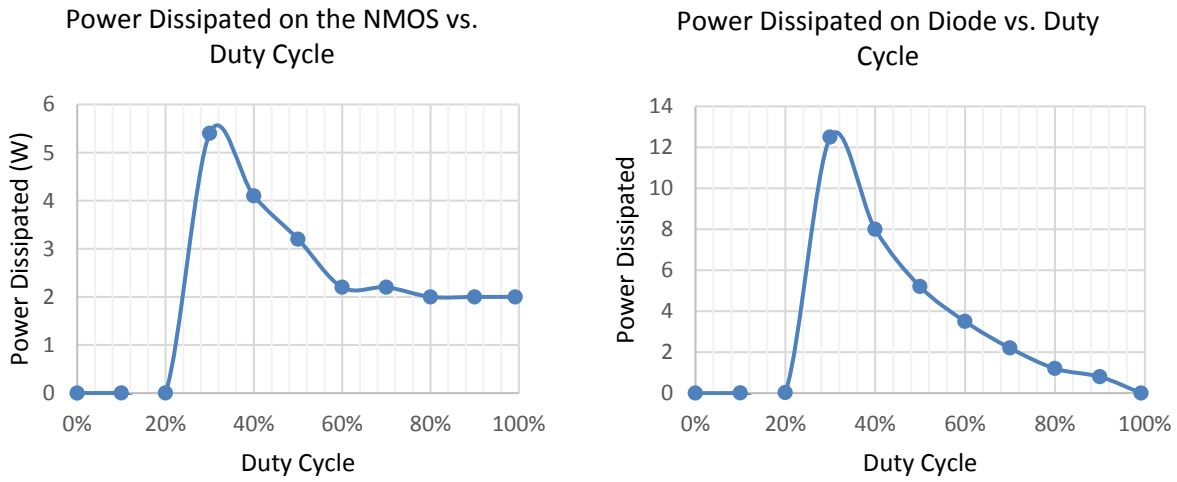

Figure 25. Power dissipated on the NMOS (left) and Diode (right)

The simulations show that our predictions calculated on the design portion of this paper, accurately reflect the simulated results on power consumption since the values obtained are well below the estimated maximum power dissipation. This validates the heat sink calculations for the NMOS and suggest the use of a heat sink on the power diode.

4.2. Current Sensors

The current sensors are an important part of the Power Point Tracking algorithm and also play a crucial role in the protective circuitry by determining values of current and sending this useful data to the microcontroller, therefore enabling the control system to work effectively.

Once the role of the current sensors in the design was highlighted, determining the appropriate type of sensors to use in the system was the next step. Since the MPPT project was sponsored by the NECAMSID lab, the MQP teams were encouraged to use IC chips manufactured by the companies that stand as members of the lab. Therefore, after analyzing a few of the options it was decided that the Hall Effect Sensors (ACS Series) from Allegro Microsystems would be most suited for the application. One of the ACS Series Allegro chips was used by the “Grid-Independent Charging Station" MQP group and proved to be a success for their design, therefore it seemed to be viable option. Once it was decided that the type of

current sensor to be implemented in the design would be a Hall-Effect sensor, it was important to understand the concept and working principle behind the technique.

In the Hall-Effect sensing technique, a beam of charged particles otherwise known as the current is passed through a conductor, which in the case of the Allegro Sensors is a copper conduction path. This current carrying conductor then generates a magnetic field that is monitored by the hall IC and converted into a proportional analog voltage. This output voltage can be interfaced and digitized via the analog-to-digital converters of a microcontroller, therefore provides an effective means of monitoring sensed current values.

4.2.1. The ACS770 Family

The Allegro ACS770 family was the first of the two families of sensor ICs that was considered for current sensing in the MPPT application. Generally, it is used for precise and accurate AC or DC current measurements. The IC is typically part of applications that entail motor control, load detection, DC-to-DC converter control, and overcurrent fault detection.

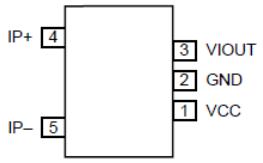

Figure 26. Pin-Out Diagram for the ACS770

The general pin layout of the ACS770 Hall-effect sensor is shown above in Figure 26. It can be clearly seen that the layout is composed of five pins and is fairly simple. The path that the sampled current follows is from IP+ (Pin 4) to IP- (Pin 5) which has an extremely low internal resistance of 100μΩ. The thickness of the copper conductive path allows the device to survive through overcurrent situations, and the terminals of this path are electrically isolated from the signal pins (Pins 1, 2 and 3). Therefore, the ACS770 family can be used in applications that require electrical isolation without prompting the need for opto-isolators or other expensive isolating components.

Table 7. ACS770 Family Table

Part Number	Optimized Range [A]	Sensitivity [mV/A]	Current Directionality
ACS770LCB-050B-PFF-T	±50	40	Bidirectional
ACS770LCB-050U-PFF-T	50	80	Unidirectional
ACS770LCB-100B-PFF-T	±100	20	Bidirectional
ACS770LCB-100U-PFF-T	100	40	Unidirectional
ACS770KCB-150B-PFF-T	±150	13.3	Bidirectional
ACS770KCB-150B-PSF-T	±150	13.3	Bidirectional
ACS770KCB-150U-PFF-T	150	26.7	Unidirectional
ACS770ECB-200B-PFF-T	±200	10	Bidirectional
ACS770ECB-200B-PSF-T	±200	10	Bidirectional
ACS770ECB-200U-PFF-T	200	20	Unidirectional

When considering the ACS770, Table 7 was analyzed using the datasheet of the product provided on the Allegro Microsystems website [14]. The current in the design follows a unidirectional path, therefore the directionality of the current sensors served to be an added feature because for the MPPT design, both cases, bidirectional or unidirectional, would serve the purpose. The MPPT system was designed for a maximum input current value of 6A and a maximum output current value of 20A. Almost all of the models of the ACS770 family, as can be seen in the table, measure a higher range of sampled current with the minimum being 50A which is beyond the range that needed to be measured in the system. Since the table shows a decreasing trend of sensitivity with an increasing current range, it was deemed appropriate to consider a different family of hall-effect sensors despite the fact that the ACS770 sensor would do the job. Therefore, a different family of sensor ICs with a lower current range was considered and is described in the next section.

4.2.2. The ACS712 Family

The Allegro ACS712 family was the second of the two families of sensor ICs that was considered for current sensing in the MPPT application. These sensors are commonly used to provide economical and accurate solutions for AC or DC current sensing and are implemented in applications like motor control, switch mode power supply, and load detection and management. After analyzing the different features of the ACS712 family of sensor ICs, one of its members was integrated in the actual design of the Maximum Power Point Tracker.

Table 8. ACS712 Family Table

Part Number	Optimized Range [A]	Sensitivity [mV/A]	Current Directionality
ACS712ELCTR-05B-T	±5	185	Bidirectional
ACS712ELCTR-20A-T	±20	100	Bidirectional
ACS712ELCTR-30A-T	±30	66	Bidirectional

Table 8 helped in the analysis of the ACS712 family and after great consideration it was determined that the ACS712ELCTR-20A-T device would be the most suitable choice. This member of the ACS712 family detects a maximum current of 20A in both directions. Although for current sensing in the MPPT application, a unidirectional sensor would also work, the added bidirectional feature proved to be advantageous. This option was chosen over the other members of this IC family because the range of current was well-suited for the design features and provided a relatively high current sensitivity of 100 $\frac{\text{mV}}{\text{A}}$ Two of these chips were integrated in the design, one for sensing current on the output side and one for sensing current on the input side.

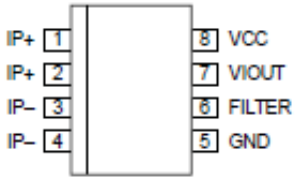

Figure 27- Pin-Out Diagram for the ACS712

The general pin layout of the ACS770 Hall-effect sensor is shown above in Figure 27. The layout is rather simple and in comparison to the ACS770 has three extra pins. There is an additional pin for IP+ (Pin 2, can be tied to Pin 1) and IP- (Pin 4, can be tied to Pin 3), which is the conductive path that the sampled current follows and a FILTER pin (Pin 6) that is not connected for the purpose of this design. The conductive path is characterized by a thick copper layer to allow for survival through overcurrent conditions and a low resistance route of 1.2mΩ to ensure that the power loss is minimized. The terminals of the path, similar to the ACS770 are electrically isolated from the signal pins (Pins 8, 7 and 5).

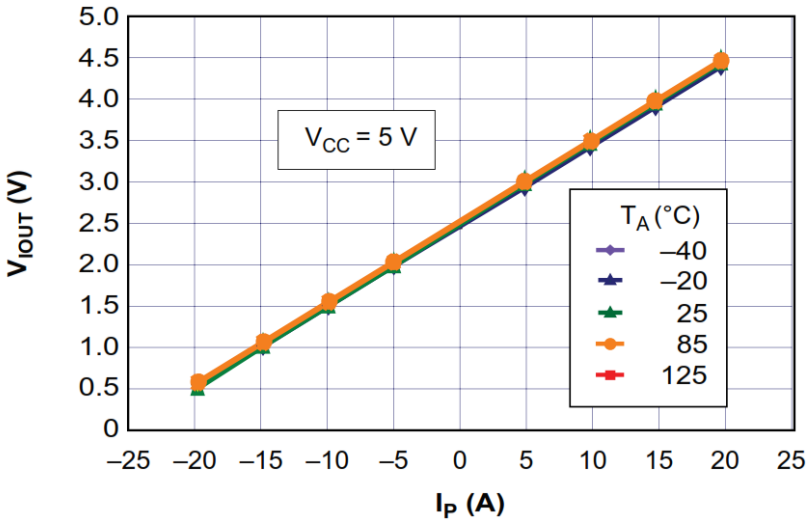

Figure 28-Output vs. Sampled Current over various Temperatures

Figure 28 above taken from the product datasheet can be used to observe how the output voltage of the sensor changes with a current swing of 40A, 20A in each direction. [15] It can be seen that the output voltage fluctuates from 0.5V to 4.5V for full range of current swing from -20A to 20A. The relationship is observed to be linear, and holds for a various range of temperatures as shown in the figure above (-40°C to 125°C). Another important deduction that can be made from the graph is that when there is no current flowing through the conduction path, or when I_P is zero, the voltage seen at Pin 7 is 2.5V. This is also known as the ideal Quiescent Output Voltage. Therefore, for an ideal situation where the quiescent voltage is $\frac{V_{CC}}{2}$, the sampled current I_P can be calculated using Eq. (22) shown below, where S is the Sensitivity:

$$I_P = \frac{2.5 - V_{measured}}{S} \tag{22}$$

The equation mentioned above, does not account for any electrical offset that may exist in the device or deviations that may possibly occur from the ideal 2.5V due to the presence of non-magnetics from external circuitry. Therefore, for more accurate current measurements, the sensors were tested by setting up the circuit shown below in Figure 29.

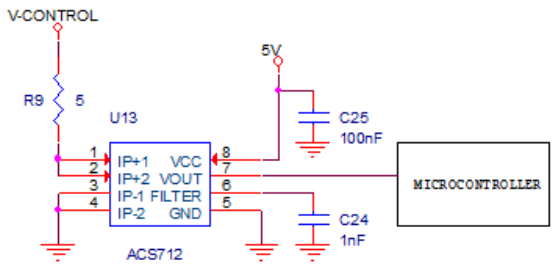

Figure 29. ACS712 Test Circuit

This test circuit proved that the voltage offset actually existed in the device and changed Eq. (22) mentioned above to:

$$I_P = \frac{2.451 - V_{measured}}{100}$$

It can be seen that a deviation of -0.049V from the nominal 2.5V was present in the device, which if not taken into account, would have given rise to inaccurate current measurements and eventually leading to an incorrect Maximum Power Point Tracking algorithm. This would have greatly affected the overall performance of the MPPT, rendering its purpose ineffective. Therefore, testing these sensors proved to be a crucial part of the design process. Once these sensors were tested, the next step was to implement them into the PCB design and interface them with the Atmega328P-PU microcontroller. Figure 30 below shows a simplified conceptual layout of the input and output sensors in the MPPT circuit interfaced with the microcontroller:

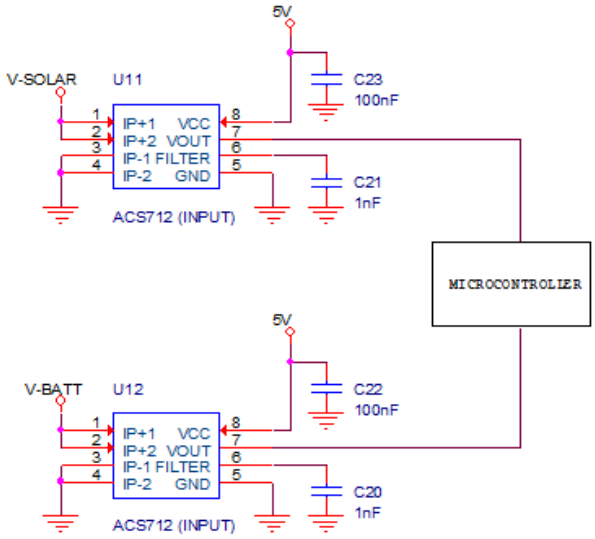

Figure 30. Input and Output Current Sensors with Microcontroller

To measure current, usually the current sensing device is placed in series to the flow of current. The same topology was observed in this case and can be seen in Figure 30. The first current sensor was added to the path of the input current, therefore in series to the solar panel. This sensor had the crucial role of reading the current values that were outputted to the microcontroller (Atmega328P-PU), where the maximum power point was monitored to successfully run the algorithm. Any inaccuracies in the measurements would greatly affect the tracking algorithm. The second sensor or the output sensor was also added in series to the battery connection to monitor the current flowing into it. This aided the protective feature of the design, as the current values that were outputted by this sensor were monitored by the microcontroller to ensure overcharge and undercharge protection of the battery and also helped in computing the power calculations on the output side hence the efficiency.

Both of the sensors are interfaced with the microcontroller, meaning that the output of these sensors are read by it, therefore, without it the sensors are essentially ineffective. The Atmega328P-PU contains an onboard 6 channel analog-to-digital (A/D) converter. The converter has a 10 bit resolution, returning integers from 0 to 1023. So the output pins of these sensors, are connected to the Atmega328P-PU's analog to digital converter. These pins allow for the analog to digital conversion of the signal output from the sensors and digitize it so the microcontroller can interpret the incoming data and use it to calculate the power and eventually run the power point tracking algorithm.

4.3. Voltage Sensor

The other type of sensors that were implemented in the Maximum Power Point Tracker were the voltage sensors. These sensors play a crucial role in the design, serving to be the epicenter of the power point tracking algorithm providing valuable data to calculate power, while also monitoring the battery voltage to ensure that the battery remains unharmed.

4.3.1. Input Sensor

The input voltage sensor monitors the input voltage at the solar panel. The sensor is a simple voltage divider that outputs a voltage based on the ratio of the resistors. The input voltage divider circuit is shown below in Figure 31**.**

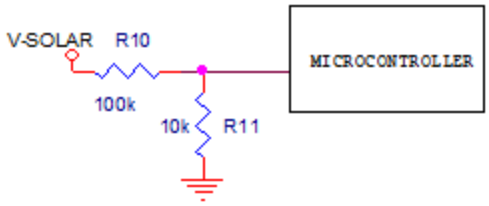

Figure 31. Input Voltage sensor

The resistors used in the voltage divider configuration were of relatively high values. This was done to ensure that the current flowing through them was limited to a small value to eventually minimize the power losses. The voltage at the solar panel varies and is dependent on factors such as the light intensity, cloud conditions, external temperature, etc. Therefore, for any value of solar voltage (V_{SOLAR}) the output of the voltage divider (V_{OUT1}) was:

$$V_{OUT1} = \left(\frac{10k}{110k}\right) V_{SOLAR} \tag{23}$$

$$\frac{V_{OUT1}}{V_{SOLAR}} = \frac{1}{11}$$

It can be seen from the above calculations that the output voltage is one-eleventh of the solar voltage. Therefore, if the solar panel operates at the rated maximum voltage point, which is around 45V, the output of the voltage divider becomes:

$$V_{OUT1} = \left(\frac{1}{11}\right)(45) = 4.09V$$

The analog value outputted by the voltage divider is read by the Atmega328P-PU microcontroller and is converted to a digital value. This digital value combined with the current value the microcontroller (Atmega328P-PU) reads and converts from the current sensor is then multiplied to compute the power and run the power point tracking technique.

4.3.2. Output Sensor

The output voltage sensor monitors the voltage at the 12V battery. The nominal voltage of the BP 20-12 battery is rated to be 12V. Because the battery is charged by the DC/DC converter and is also connected to a load, this nominal voltage can fluctuate depending on various conditions. If the battery is being charged, while no load is connected, the voltage at the output can easily exceed 12V. According to the datasheet of the BP 20-12 battery, the highest tolerable voltage is 14.1V after which the battery does not function effectively. Also, if the system is being used at night when there is no charging but a load is

connected to the battery, the battery can potentially be drained, dropping the voltage across it to a very low value. Based on the datasheet this lower threshold is 11.1V [16].

Therefore, it was important to identify these upper and lower thresholds in order to design an effective and purposeful voltage sensor. These thresholds are limiting values that prompt the microcontroller to take the necessary steps that can help prevent serious damage to the device. The output voltage sensor itself is a simple voltage divider that outputs a voltage based on the ratio of the resistors. The circuit for this can be seen below in Figure 32:

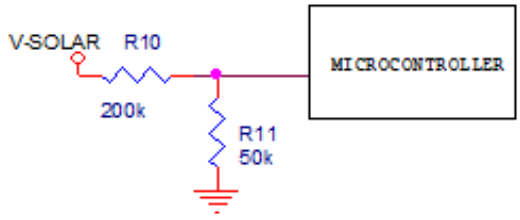

Figure 32. Output Voltage Sensor

Similar to the voltage divider at the input side, the output voltage divider also makes use of resistors that are of high values to ensure that the current flowing through them is meniscal. This is done to minimize power losses. The general voltage divider equation is then derived based on the configuration shown in Figure 9. The relationship between the output voltage (V_{OUT2}) and the battery voltage (V_{BATT}) becomes:

$$V_{OUT} = \left(\frac{50k}{250k}\right) V_{BATT} \tag{24}$$

$$\frac{V_{OUT}}{V_{BATT}} = \frac{1}{5}$$

It can be seen from the above calculations that the output voltage is one-fifth of the solar voltage. If the battery is at the nominal value of 12V the output voltage is:

$$V_{OUT} = \left(\frac{1}{5}\right)(12) = 2.4V$$

At the upper threshold value, the voltage outputted by the sensor is:

$$V_{OUT} = \left(\frac{1}{5}\right)(14.1) = 2.82V$$

Therefore, when the output of the voltage sensor 2.82V, the microcontroller must take the necessary action to reduce the voltage across the battery to prevent overcharging. This is done using software

through which the duty cycle of the PWM is adjusted in order to reduce the rate at which the battery is charged.

At the lower threshold value, the voltage outputted by the sensor is:

$$\mathrm{V_{OUT}} = \left(\frac{1}{5}\right)(11) = 2.2\mathrm{V}$$

Therefore, when the output of the voltage sensor 2.2V, the microcontroller (Atmega328P-PU) must take the necessary action in order to prevent the battery from being drained or undercharged by isolating the load or if the conditions permit increasing the duty cycle to charge the battery faster. This is controlled using software as well. If undercharging occurs during the night the only way to deal with this issue is by trigging the protective circuitry and the relay to isolate the battery so no more current is drawn from it.

The analog values outputted by both the voltage sensors are read by the microcontroller and digitized using its Analog-to-Digital converter. These digital values combined with the current values that are read through the sensors are then multiplied to compute the power values which are then used in the power point tracking algorithm.

4.4. High Side MOSFET Driver

In order to achieve a low conduction resistance with the NMOS, the Gate to Source voltage V_{GS} has to be sufficiently high but lower than the breakdown voltage (voltage at which the oxide insulator breaks down and hence the MOSFET breaks). The datasheet of the device suggests $V_{GS} = 10V$ for a good switching operation. However, the voltage at the source of the NMOS with respect to the common ground is always equal to the voltage across the battery which in this case is approximately 12V. The peak to peak amplitude of the PWM waveform outputted by the microcontroller (Atmega328P-PU) is 5V thus, the need of a driver circuit capable of boosting the voltage to 10V with respect to the source of the MOSFET. One way to do so is by having an isolated power supply for the logic circuitry (whose ground would be the source of the MOSFET) and then using a simple buffer to amplify the 5V signal to 10V. However, this implies more complexity and a whole design that could take a lot of resources and time. Integrated circuits have already been designed for driving the high or low state of a MOSFET (NMOS or PMOS), these are called *High Side Drivers or Low Side Drivers* respectively. This is the case of the IR2117 from International Rectifier. The IR2117 is a High Voltage IC designed for driving high speed MOSFETs and IGBT with a high pulse current at its output. Its main operation is based on an external bootstrap capacitor that is charged during the low state and then discharged during the high state producing the required gate to source

voltage. This external capacitor is crucial for the operation of the high side driver. Figure 33 shows the typical application of the IR2117 [17].

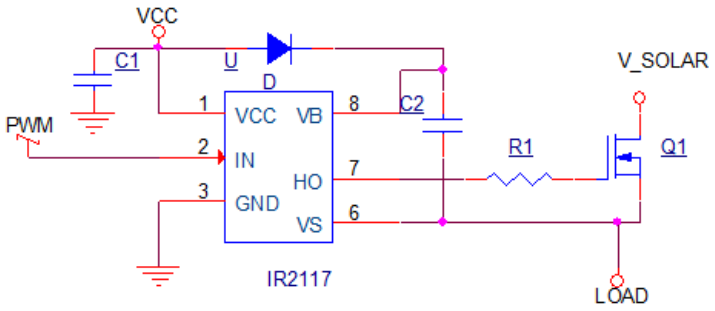

Figure 33. Typical high side driver configuration

For resistive and capacitive loads, the capacitor charges through it however, for charging applications neither the diode of the dc to dc converter nor the load (the battery) can charge the capacitor since Vs is kept at the battery voltage which in this case is 12V. This was proven by implementing the suggested circuit and in fact, the capacitor did not charge and hence the high side driver did not operate. The solution is to use a resistor to charge up the capacitor. The voltage at the pin V_B is always approximately equal to $V_{CC} - 0.7V$, therefore connecting a resistor from the drain of the MOSFET (higher than V_{CC}) to V_B generates a current that flows through it equal to $\frac{(V_D - V_B)}{R}$ and hence the capacitor is charged by a current source equal to $\frac{(V_D - V_B)}{R} - I_B$ where I_B is the quiescent current flowing through the pin V_B. According to the application note for the AN-978 [18], the average current flowing through this resistor has to be at least 1mA. Which implies:

$$\frac{(V_D - V_B)}{R} = \frac{(V_{SOLAR} - (V_{CC} - 0.7))}{R} \geq 1mA \tag{25}$$

Since the driver circuit is going to be powered by the battery externally connected, $V_{CC} = 12V$. Given a fixed value of V_{SOLAR}, the maximum value of R can then be easily calculated. However, this charging application does not have a fixed input voltage V_{SOLAR}. Instead, that voltage is ideally aimed to vary from 48V (open circuit voltage, 0% duty cycle) all the way to the voltage across the battery (100% duty cycle). Two main considerations are important, first, the bootstrap capacitor (connected from VB to VS) charges during the low state of the PWM which means that as the duty cycle increases, the charging time decreases. Second, as the duty cycle increases, V_{SOLAR} decreases and as a consequence the current that charges the capacitor gets diminished. This is key to understand that the driver circuit will never be able

to work with a duty cycle of 100%. The aim is to achieve a wide range for the duty cycle so that the Maximum Power Point can be effectively tracked. Assuming that the voltage across the solar panel can be as low as 16V at the highest reached duty cycle, the resistor is found to be:

$$R \leq \frac{(16 - (V_{CC} - 0.7))}{1mA} = 4.7k\Omega$$

The issue of charging the capacitor using the charging resistor is that the voltage across the capacitor can be pretty high (since this voltage would be directly proportional to the low state time) and therefore, the gate to source voltage applied to the MOSFET would likely be higher than the maximum rated voltage and would break the device (and possibly the capacitor as well). This issue was properly addressed by adding a 12V Zener diode in parallel with the capacitor. This regulates the gate to source voltage applied to the gate to the device preventing it to be more than 12V. The final driver circuit is shown in Figure 34.

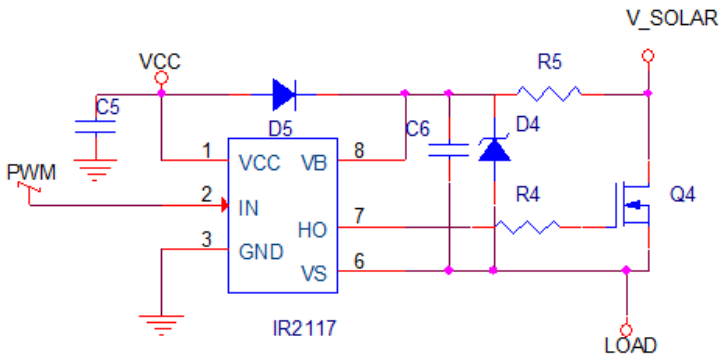

Figure 34. Modified high side driver circuit for charging applications

4.5. Protection Circuitry

There are three different issues that need to be properly addressed in order to prevent the system from breaking down. First, once the battery is fully charged, the output current of the DC to DC converter has to be decreased in order to maintain the voltage across the battery constant just for restoring the lost charge due to leakage and external devices connected to the system. Second, if the battery is about to get completely discharged and the output current of the DC to DC converter is lower than the current drawn by the load, the system has to disconnect the load to prevent the damage of the battery. Third, if the battery is disconnected, there must be an action to prevent the MOSFET from switching, otherwise the voltage at the output would increase linearly and hence damage the system (the battery acts as a

voltage regulator keeping the output of the DC to DC converter approximately fixed). The voltage across the terminals of a lead acid battery varies depending on the state of the battery. When fully charged, this voltage is approximately equal 14.1V for many 12V car batteries. Similarly, when the battery is approaching a deep discharge state, this voltage decreases to approximately 11V. Monitoring the voltage across the output of the DC to DC converter is then vital since it contains information regarding the battery. The first and third situations can be controlled by the duty cycle of the switching waveform; once the battery is fully charged, the duty cycle is decreased up to a point (greater or equal than zero) when the voltage across the battery remains at 14.1V. The following pseudo code describes the way to maintain the charge of the battery without overcharging it:

```
//Monitor Overcharge
voltage_out=Read voltage across the battery;
if (voltage_out>=14.1)
{
      yes: reduce duty cycle;
      no: do nothing;
}
```

If the voltage across the battery gets as high as 15V, this could mean that the battery has been overcharged, damaged or even that the battery has not been connected and hence it is really important to stop switching which means setting the duty cycle equal to zero. The pseudo code can then modified as follows,

```
//Monitor Battery
voltage_out=Read voltage across the battery;
if(voltage_out>=15)
{
      yes: duty cycle=0;
      no:   if (voltage_out>=14.1)
            {
                  yes: reduce duty cycle;
                  no: do nothing;
            }
```

The second situation however, cannot be controlled by software only since it involves disconnecting the external load automatically. This can be done using a relay activated by the microcontroller. Again, there is a need for a circuit in order to drive the coil of the relay. This can be simply designed with a NPN BJT, a resistor to limit the current at the base and a freewheeling diode that prevents from having high peak voltages transients due to the coil of relay. This circuit can be seen in Figure 35.

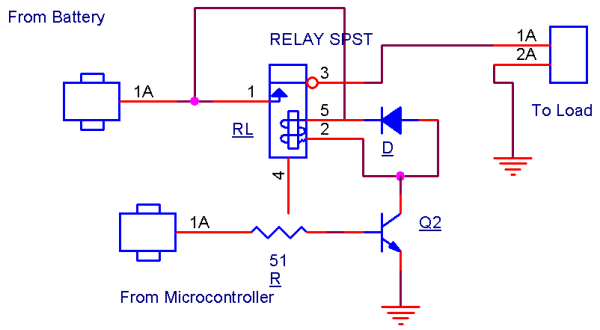

Figure 35. Under voltage protection

The relay used in order to implement this circuit is the G8N1 from OMRON whose coil nominally works at 12V and 53.3mA. Since the coil current is relatively low, the common 2N3904 NPN transistor and the 1N4148 diode can handle the task. The resistor R has to be low enough to drive the BJT to the saturation region so, 51Ω would meet that requirement. The software is described with the following pseudo code.

```
//Undercharge

If(voltage_battery<threshold)

{

      Yes: deactivate relay

      No: keep relay activated

}
```

4.6. Software

The software algorithm served to be the backbone of the Maximum Power Point Tracker. The algorithms that are mentioned in this report were analyzed and explored but were never implemented for the purpose of this project. Rather a slightly modified version of the Perturb and Observe technique was used. This modified algorithm involves sweeping the duty cycle of

the PWM that controls the MOSFET, from 0% to 90% in increments of 5%. While sweeping through this range of values, power calculations are made and recorded with each increment. Once the duty cycle reaches 90%, it gradually decreases and eventually stops at the duty cycle value where the maximum power point is recorded. The algorithm repeats itself and sweeps the duty cycle from 0% to 90% once the current sensors detect a change in current, if no change is sensed the duty cycle remains at the value at which maximum power is observed. The block diagram for the algorithm is shown below in Figure 36:

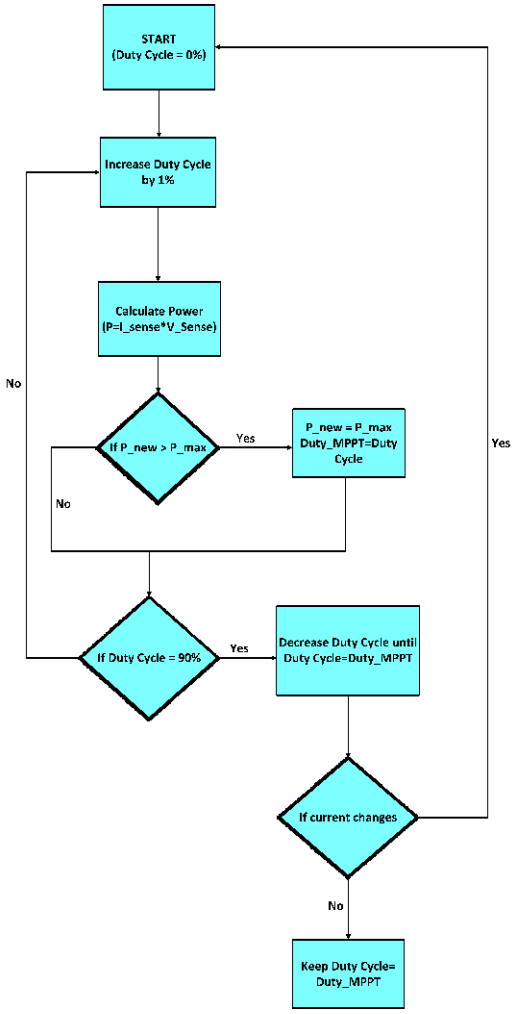

Figure 36. MPPT Algorithm

The algorithm may not be the most efficient way to track power but is certainly effective. A drawback of implementing this algorithm is certainly the time that is required to sweep the duty cycle. Also, on a day of constantly changing external conditions, the current may change rapidly

causing the algorithm to keep repeating itself essentially reducing the efficiency of maximum power point tracking.

4.7. Schematic Diagram and PCB for the design

The circuit design of the Maximum Power Point Tracker is shown in Figure 37 below. The schematic is an overview of the circuit that was used to determine the layout of the Printed Circuit Board. It was compiled using the Cadence OrCAD Capture software and the PCB Editor software (part of the Cadence package) was used to work on the board layout. The figure shows the different components integrated in the design and the connections between them. Making sure the circuit was accurate and reflected the actual design of the MPPT that was initially tested on a breadboard, was crucial. This was because the schematic later served as a reference when designing the two-layer PCB for the design (shown in the Appendix 9.3). Therefore, justifying the need for each component, ensuring that electrical ratings were not exceeded and researching on the availability of each component were the main tasks that were accomplished prior to finalizing this schematic. Designing the footprints for the components shown in the schematic also proved to be a tedious yet significant step in completing the circuit design. Once the footprint was designed for each component, it was scrutinized and double-checked to see if the size of the holes and distances between the pins matched with the datasheet. These footprints were then added to the corresponding components in the schematic shown in Figure 37 below:

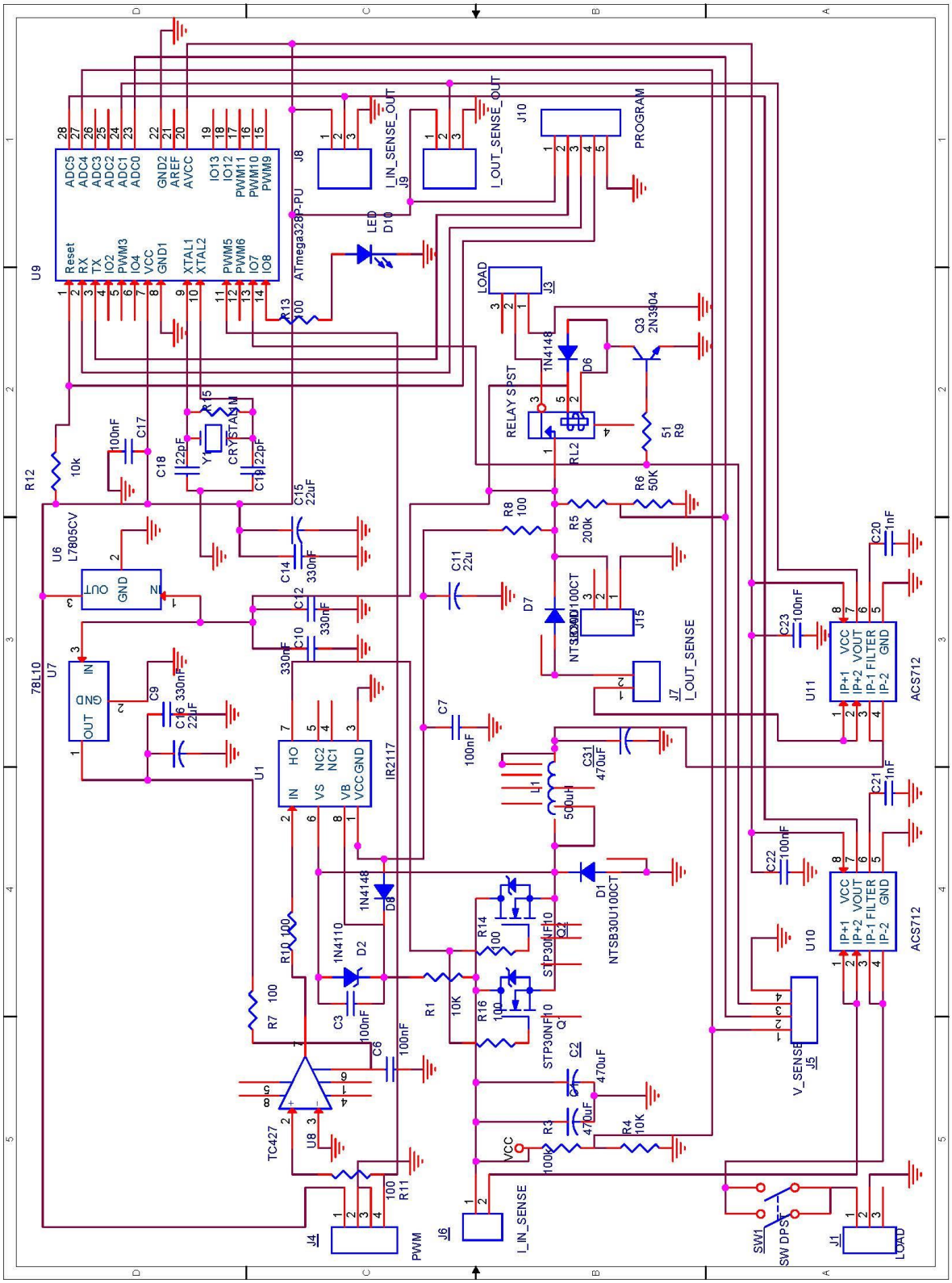

Figure 37. Schematic of Complete Design

One of the most important aspects of the design shown below is it contains a Plan B. This Plan B would come into play if one of the main components on board failed to work. The main components include the Atmega328P-PU microcontroller with its associated circuitry, the input current sensor and the output current sensor. The way this fault proof technique worked was through the many connectors the PCB had on board. These connectors could be externally interfaced if needed and would provide the same path for the signal or current. But fortunately they were not used at all and the components worked effectively in the PCB layout. The final PCB design is shown below in Figure 38.

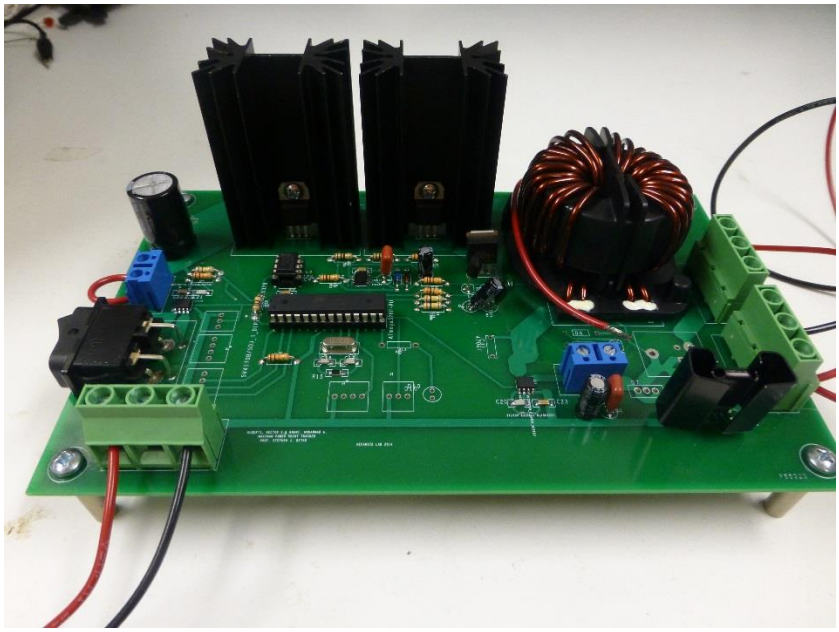

Figure 38. Final PCB Design

5.0. MEASUREMENTS AND RESULTS

The Maximum Power Point Tracking algorithm implemented in the system is based on sweeping the duty cycle from 0% to the maximum duty cycle allowed by the high side driver (approximately 90% depending on the weather conditions). This algorithm as explained in greater detail in Chapter 4, keeps track of the power calculations in the system. This sub-section mainly focuses on discussing the results obtained from testing this algorithm in the MPPT system. Figure 39 contains some oscillograms captured as the algorithm was being performed. Notice that the duty cycle increases and then settles down at the MPP duty cycle.

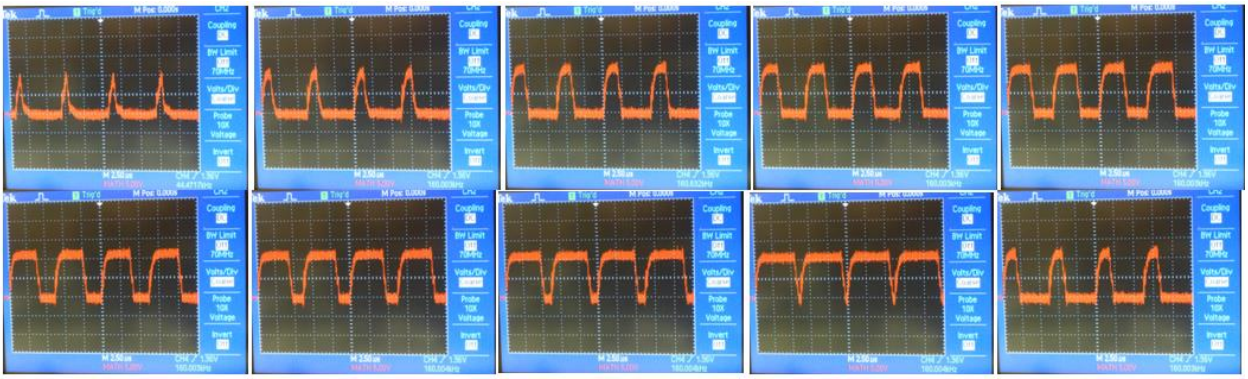

Figure 39. Duty cycle sweeping

The change in duty cycle involves the change of the voltage across the solar panel. Which, was first assumed to be a linear function of the duty cycle, but then it was shown by the simulations that the relationship can be modeled by a sixth degree polynomial and not as a straight line. The measurements taken during different weather conditions present a similar nonlinear behavior. Figure 40 shows the Duty cycle-Voltage graph obtained on the measurements taken on March 16th, 2014 at 3:40 pm.

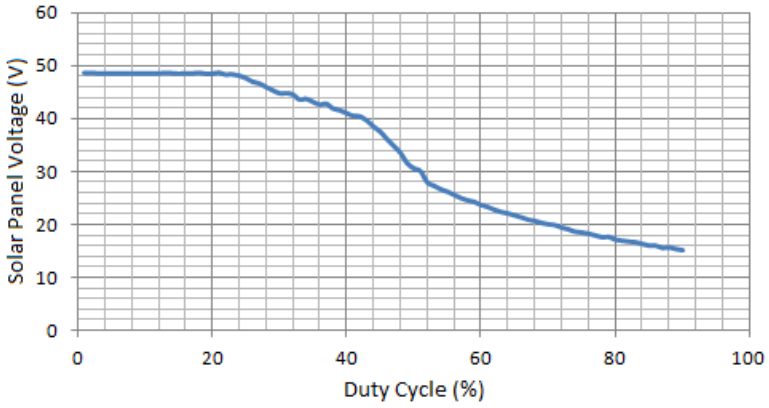

Figure 40. Variation on Voltage as a function of duty cycle

The shape of the Duty cycle - Voltage graph is comparable with the one obtained with the simulated data. The input voltage, the output current, the ripple voltage and ripple current are not a linear function of the duty cycle as assumed in the main design. This was proven not only with the simulations but also with the measurements taken in different conditions. This non linearity does not affect the operation of the Maximum Power Tracker. In fact, according to Figure 40, sweeping the duty cycle changes the voltage across the solar panel and hence moves it along the VI curve.

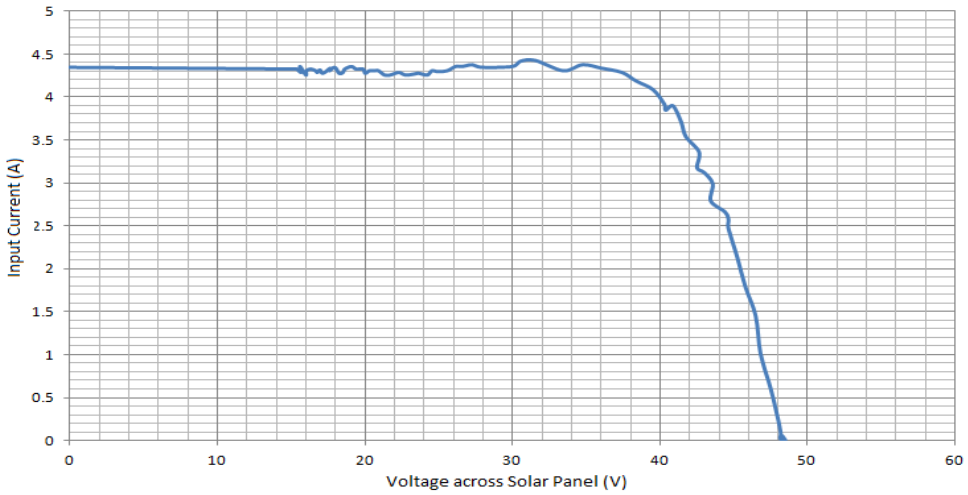

Figure 41. Current vs. Voltage curve corresponding to the solar panel at 3:40pm

As the voltage moves along the VI curve, this allows obtaining the VI characteristics of the solar panel corresponding to the moment when the sweeping takes place and hence the point where the maximum power is obtained. Figure 41 contains the Voltage-Current characteristics obtained on the same date and time as mentioned above.

The performance of the solar panel mainly depends on the sun intensity and temperature. Hence, different VI curves can be obtained at different times during the day. When light conditions change, a new curve is obtained and the new Maximum Power Point is tracked. Those changes in light intensity conditions are read by the system as a change in current at a fixed duty cycle, when this occurs, the systems sweeps the duty cycle again. However, it is important to take into consideration that the system does not have to react to relatively small changes in current since those can be due to noise on the measurements taken by the ACS712 or input ripple current.

To see how the system reacts to changes in light conditions eventually leading to changes in current, measurements were taken at different times throughout the day on March the 16th, 2014. The values read from the sensors corresponding to the input voltage, input current, output current and output

voltage were sent via serial interface to the computer and processed to obtain the VI curves shown in Figure 42.

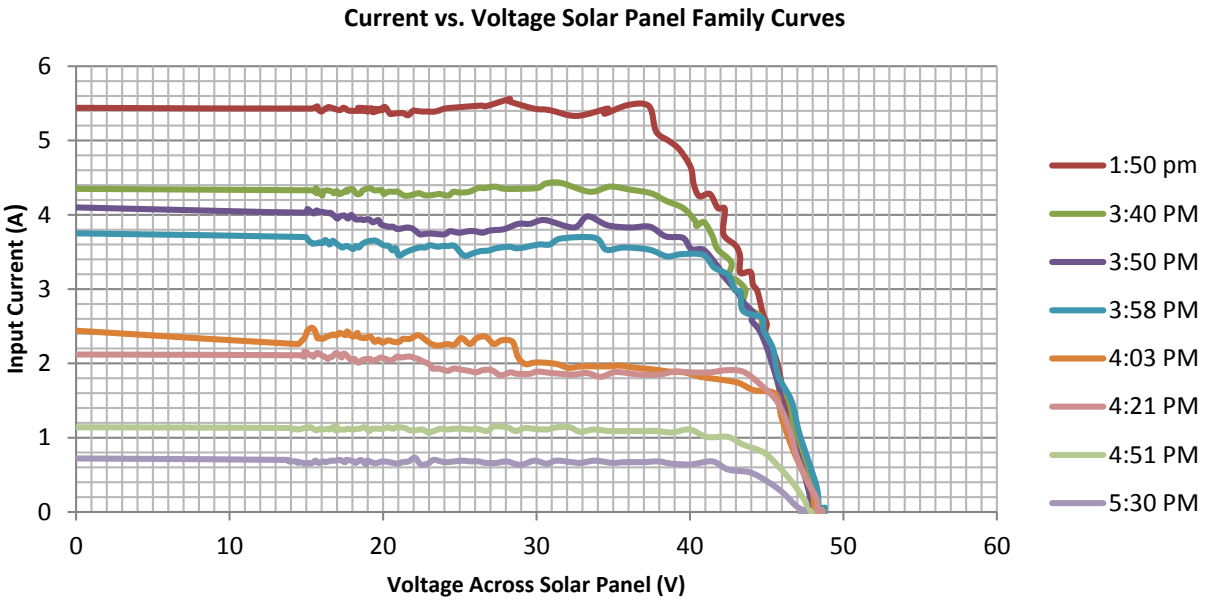

Figure 42. Voltage-Current family of curves corresponding to different light conditions

The above figure shows how the VI characteristics of the solar panel change over the course of a day. Although the system is only capable of sweeping the voltage across the solar panel from approximately the battery voltage (12V) to the open circuit voltage (48V), the curves also include the data point $V = 0V$ and $= I_{SC}$. The short-circuit current I_{SC} was measured using an ammeter with the MPPT disconnected right before using it to obtain the other data points.

It is evident from the graph above that the current at which the solar panel operates at changes quite frequently. These measurements were taken in the span of three hours and forty minutes and eight different VI curves were obtained. As expected, the current at which the solar panel operates decrease over the progression of the afternoon due to the decrease in light intensity. Those changes in light intensity invoke changes in power delivered by the solar panel. This can be clearly seen in Figure 44.

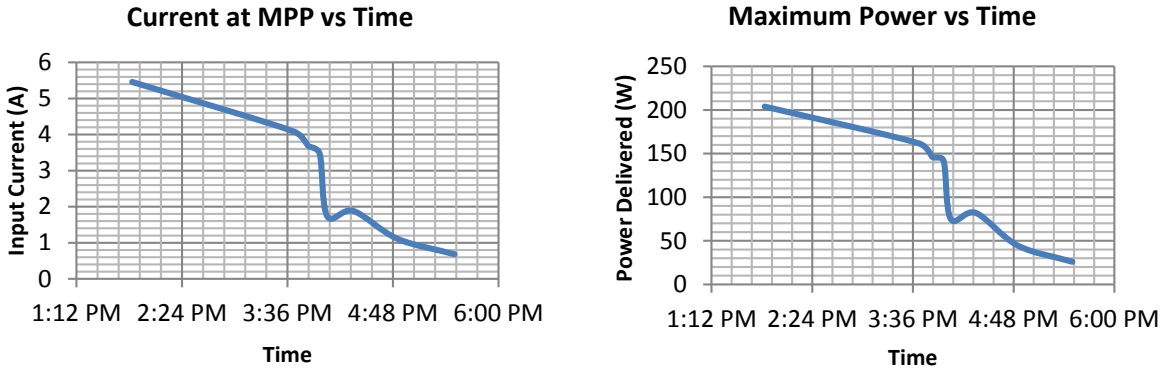

Figure 43. Changes in current and power over the afternoon on March 16th, 2014

Both graphs shown above in Figure 43 (Current vs. Time and Maximum Power vs. Time) seem to follow a very similar behavior which depends on the light intensity outside. Since, dividing the power by the current at the input results on the voltage across the solar panel, both graphs suggest that the Maximum Power Point was located in a relatively small range of values. This can also be seen on the graphs of Power as a function of Voltage shown in Figure 44 corresponding to the same measurements as the previous graphs.

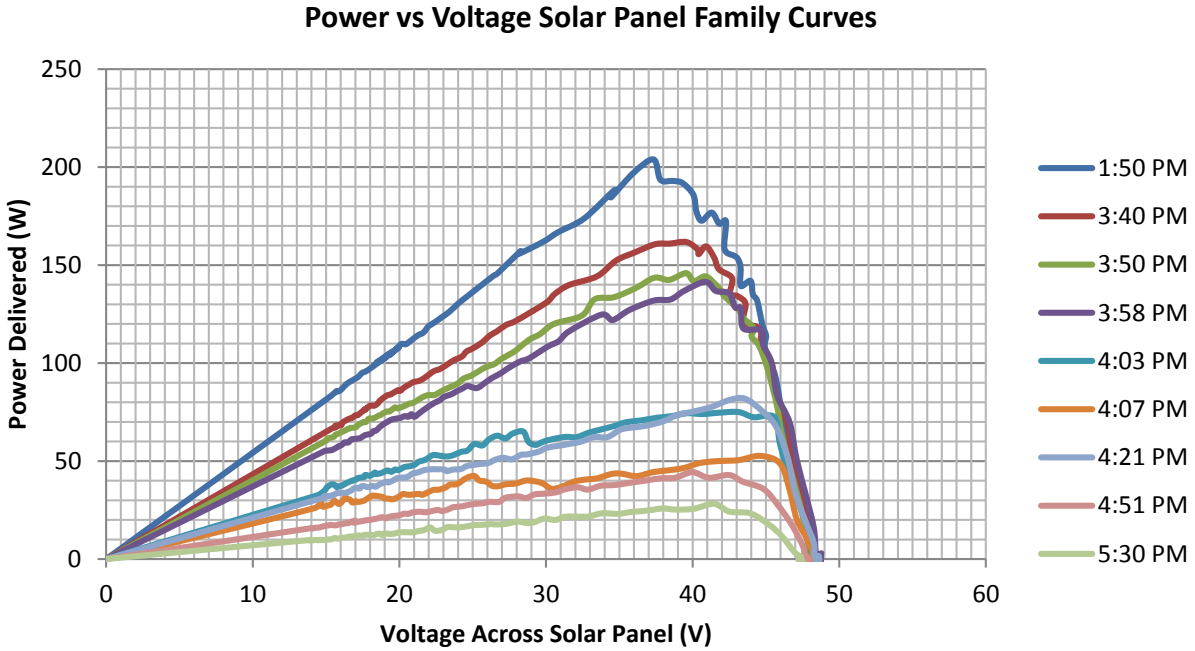

Figure 44. Power-Voltage curves obtained on March 16th, 2014.

Again notice that the data point $V = 0V$ and $P = 0W$ corresponding to the short-circuit operation has been added in order to complement the graph. The Power-Voltage curves are quite similar to the expected behavior of any solar panel and as expected, there is a unique maximum power point that corresponds to a unique voltage across the solar panel. From the graph it can be seen that the Maximum Power Point at each curve corresponds to a different voltage across the solar panel. This also suggests a different duty cycle and hence the need for constantly sweeping it to obtain the new MPP.

6.0. FUTURE WORK

A technical design is always restricted by time, budget and resources. This is a pragmatic dilemma that engineers and individuals from many other professions encounter in real world scenarios. This MPPT project experience provided a similar challenge and dealing with these restrictions affected the design of the project and overall outcome. While the existing design of the Maximum Power Point Tracker proved to be a success, some technical and aesthetic features could be improved to increase educational value, compatibility and compactness of the product and can also serve to be the basis of future contributions and projects in the energy discipline.

6.1. Design Modifications

The software incorporated in the design involved sweeping the duty cycle of the PWM supplied to the MOSFET, from 0% to 90% and locating the maximum power point during this cycle. This was the only algorithm tested and theoretically wasn't the most efficient one. Testing multiple algorithms and finding the most efficient way to track the power point or even running a few in parallel could serve as a future contribution to this project and can greatly improve the software design.

A technical improvement in the design could be using a synchronous buck converter instead of the non-synchronous buck converter. A synchronous converter makes use of two switching devices. The switch in the case for the MPPT design was a MOSFET. The synchronous converter is a trade-off between added cost and improved efficiency. The efficiency is improved by removing the diode, hence removing the voltage drop across it. Therefore, adding a second MOSFET with a small ON resistance can greatly improve the efficiency of the buck converter and can be part of a future project.

The MPPT design uses a switch to isolate the solar panel from other circuitry. The switch is capable of handling high currents and voltage, but the solar panel is isolated from the circuit (switch is open) the other components and ICs are still powered through the battery, therefore an improvement to this could be adding another switch on the battery side that could isolate the battery from the circuit as well so that when both switches are open, the main circuitry and components are not powered. This can help improve the efficiency of the system. Also, another

design modification can be adding a push button switch that resets and forces the algorithm to start over again. This technique could help in removing transients that may be caused in the system.

6.2. PCB Revision

The Maximum Power Point Tracker was designed on a Printed Circuit Board (PCB). Modifying and making the PCB layout more compact and effective can serve to be a design modification. The PCB design performed well and served its purpose but some components on the board could use more space. For example, the power diode has a voltage drop across it which at high current values (around 5A) causes high power dissipation, eventually heating it up. Although the design still worked, this issue could be resolved using a heat-sink, which required more space and modification of the PCB layout.

6.3. Educational Value and Aesthetics

The Maximum Power Point Tracking device is a unique design that serves the power industry and helps in improving efficiencies of solar energy harvesting devices. With the current energy crisis the world faces, it may be a possibility that this design is eventually mass produced. And an important part of mass production is aesthetics. An aesthetically pleasing and compact product is more likely to sell. Currently, the MPPT design is on a printed circuit board (PCB), so a future task for students could be working on physical features of the design or incorporating a plastic enclosure to it that could add aesthetic value making it more marketable.

The MPPT design was meant to be incorporated in the “Grid-Independent Charging Station” MQP which educated the common visitor in the Atwater Kent building about power flow through the system, from the solar panel to the battery and load. While this gave a good overview of the system, an educational yet more informative feature that could be added to the project can involve a serial interface via the Arduino and a LCD that when connected to a computer or TV, shows the visiting public or students the algorithm working in real-time by graphing the power against voltage curve and displaying it on the screen. This would allow visitors to see how the algorithm is affected by external factors such as temperature and sunlight. Adding on to this feature would be a more technical aspect of the power point tracking algorithm.

6.4. Summary

It can be clearly seen, that there are many sub-projects or tasks that can emerge from the design of the Maximum Power Point Tracker, which means there is room for improvement. No design is ever perfect, and there are always ways in which it can be made more efficient, marketable and attractive to its targeted audience, by either adding to cost, increasing timeframe or even altering the scope of the project. Most of the modifications mentioned above could not be carried out mainly due to time constraints but they still have the potential to be pursued as future projects, inevitably forcing more work to be done in the renewable energy discipline, which in essence was one of the main goals of this MQP.

7.0. CONCLUSIONS

The Custom MPPT project promotes renewable energy applications and encourages students within the ECE department to take on the challenges that directly or indirectly deal with this field. This discipline of electrical engineering demands immediate concern given the energy problems the world currently faces. Research and development in this area of study may be tedious and require substantial technical efforts but nonetheless, it is an area that holds the key to a cleaner and sustainable future.

This project successfully tackled the problems that come with working with applications involving power and energy. Throughout its duration many practical challenges were faced mirroring real world and industrial scenarios. From applying circuit theory, to designing a PCB layout to testing and evaluating circuitry using different simulation tools; the project overall provided exposure to a variety of technical disciplines. The fundamentals of power electronics, microelectronics, and controls engineering were all applied to the power system developed as part of this project.

The final design is a fully functional circuit board incorporated in the “Grid Independent Charging Station” MQP that successfully delivers its set goals. However, different features and design aspects such as measurement accuracy, efficiency, and aesthetics can be improved upon. This always provides for future work and innovation that can be the focus of the bright minds that decide to take on the challenge and help contribute significantly towards this challenging field.

8.0. BIBLIOGRAPHY

[1] A. Ducimo, K. Snieckus and N. VerLee, "Renewable Energy Applications," Worcester Polytechnic Institute, Worcester, April 2012.

[2] S. Veilleux and A. Delphia, "Grid-Independent Charging Station with Power Flow Display," Worcester Polytechnic Institute, Worcester, December 2012.

[3] EPSolar, "The Tracer 2210RN," [Online]. Available: http://www.belismart.com/20a-12v-24v-tracer-2210rn-mppt-solar-controller.html.

[4] SunSaver, "SS-MPT-15L," [Online]. Available: http://www.wholesalesolar.com/pdf.folder/controller%20pdf%20folder/sunsavermppt.pdf.

[5] SunSaver, "The MorningStar MPPT," [Online]. Available: http://www.eco-distributing.com/Morningstar-TriStar-TS-MPPT-45-Controller-122448V-45Amp_p_678.html#.

[6] E. Trishan and P. L. Chapman, "Comparison of Photovoltaic Array Maximum Power Point Tracking Techniques," *IEEE TRANSACTIONS ON ENERGY CONVERSION,* vol. XXII, no. 2, pp. 439-449, 2007.

[7] C. Liu, B. Wu and R. Cheung, "Advanced Algorithms For MPPT Control of Photovoltaic Systems," Toronto, Ontario, 2004.

[8] N. Mohan, "Power Electronics: A First Course," in *Power Electronics: A First Course*, Minneapolis, Wiley, 2012, p. 43.

[9] R. Nowakowski and N. Tang, "Efficiency of synchronous versus nonsynchronous buck converters," *Analog Applications Journal TI,* pp. 15-18, 209.

[10] R. F. Nelsona and M. A. Keprosb, "AC Ripple Effects on VRLA Batteries in Float Applications".

[11] Schaffner, "Current Compensated Chokes Datasheet," Octuber 2012. [Online]. Available: http://www.schaffner.com/en/products/datasheet-high-res/product/rb-series-common-mode-chokes.html.

[12] ON Semiconductors, "NTSB30U100CT Datasheet," January 2013. [Online]. Available: http://www.onsemi.com/pub_link/Collateral/NTST30U100CT-D.PDF. [Accessed 29 January 2014].

[13] STMicroelectronics, "STB30NF10 Datasheet," June 2006. [Online]. Available: http://www.st.com/st-web-ui/static/active/en/resource/technical/document/datasheet/CD00002440.pdf. [Accessed 20 December 2013].

[14] Allegro Microsystems LLC, "ACS770," [Online]. Available: http://www.allegromicro.com/Products/Current-Sensor-ICs/Fifty-To-Two-Hundred-Amp-Integrated-Conductor-Sensor-ICs/ACS770.aspx.

[15] Allegro Microsystems LLC, "ACS712," [Online]. Available: http://www.allegromicro.com/Products/Current-Sensor-ICs/Zero-To-Fifty-Amp-Integrated-Conductor-Sensor-ICs/ACS712.aspx.

[16] BP Series Batteries, "B.B 20-12," [Online]. Available: http://www.bb-battery.com/productpages/BP/BP20-12.pdf.

[17] International Rectifier, "IR2117 Datasheet," 14 May 2007. [Online]. Available: http://www.irf.com/product-info/datasheets/data/ir2117.pdf. [Accessed 21 December 2013].

[18] Iternational Rectifiers, "HV Floating MOS-Gate Driver ICs," 23 March 2007. [Online]. Available: http://www.irf.com/technical-info/appnotes/an-978.pdf. [Accessed 25 January 2014].

9.0. APPENDICES

9.1. Project Schedule

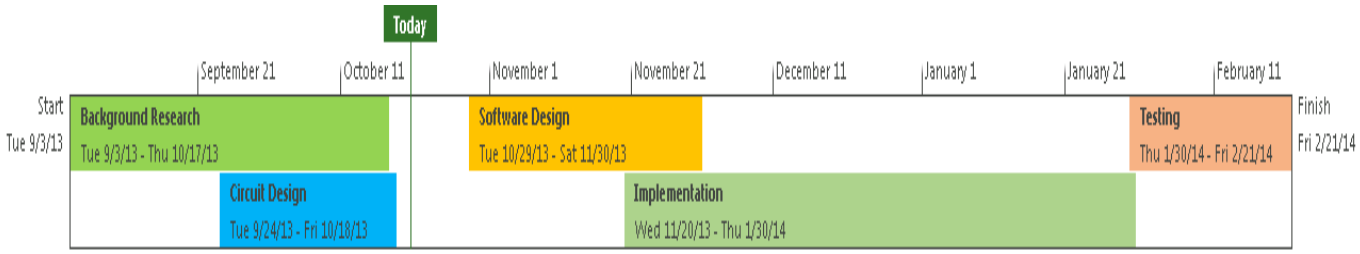

ID	Task Name
1	**Background Research**
2	Previous Projects
3	MPPT Operation
4	MPPT Algorithims
5	Buck Converter Topology
6	**Circuit Design**
7	DC/DC Converter Design/Simulation
8	DC/DC Converter Part Selection
9	Circuit Protection Design
10	**Software Design**
11	Microcontroller Selection
12	MPPT Algorithim Program
13	Sensor Code
14	LCD Display
15	Debugging
16	**Implementation**
17	PCB Design
18	Circuit Integration
19	**Testing**
20	Hardware
21	Software
22	Circuit Performance

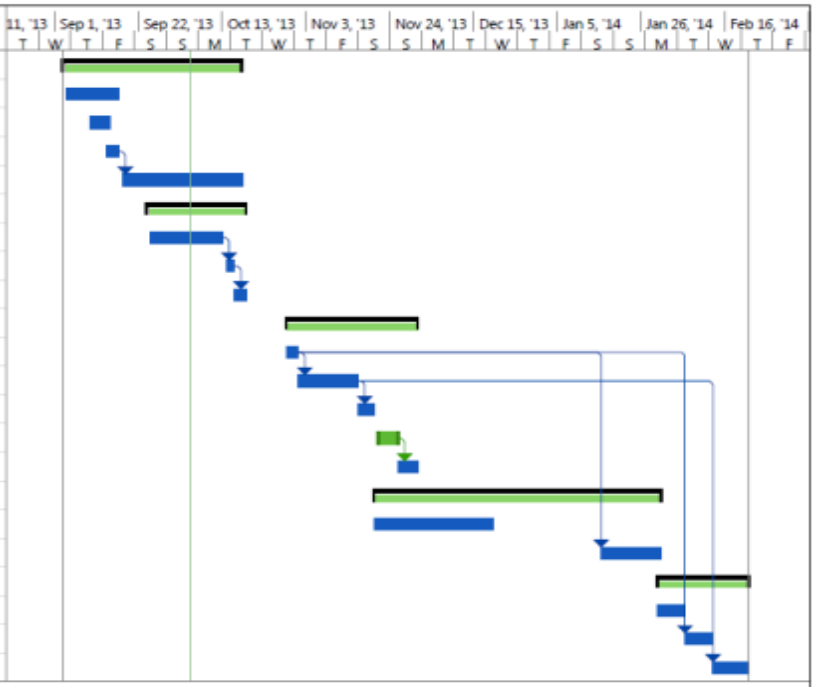

Custom Maximum Power Point Tracker

Advisors
Stephen J. Bitar
John McNeill

Hector E. Alberti Arroyo
Mohammad A. Ghani

New England Center for Analog & Mixed Signal Design

Goals

- Promoting use of renewable energy for potential future projects.
- Displaying voltage, current and power through LCD for educational purposes.
- Maximizing output power using tracking point.
- Minimizing switching losses.
- Ensuring compatibility with off grid station project from previous MQP.

Block Diagram of Design

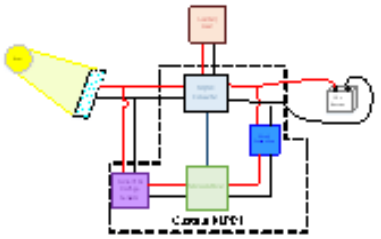

Project Schedule

- This project is to be completed in three terms namely A, B and C-term.
- Below is a Gantt Chart that shows in detail the length of each phase and task of the project:

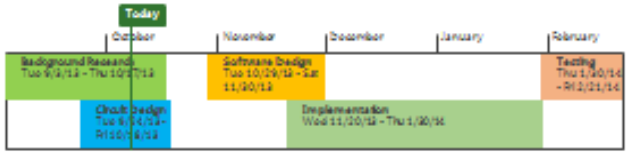

Technical Challenges

- Designing circuitry to control and stabilize voltage across the solar panel.
- Controlling high peak fluctuations during transient.
- Implementing the control loop for the DC/DC converter.
- Designing overcharging and undercharging protection for the battery.

Features

- Maximum power point tracking.

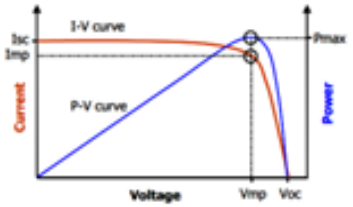

- Overcharge/undercharge circuit for battery protection.
- Control loop to ensure low peak fluctuations during transient.
- LCD display for educational purposes showing how PWM affects voltage operation point and hence output power.

Current Progress

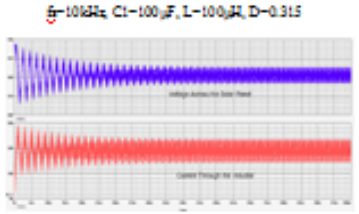

Effect of switching frequency
fs=100kHz, C1=100 µF, L=100 µH, D=0.315

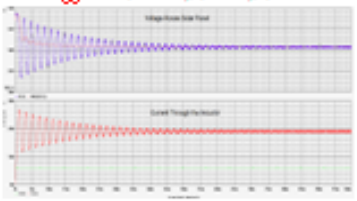

Effect of Capacitor C1
fs=100kHz, C1=1000 µF, L=100 µH, D=0.315

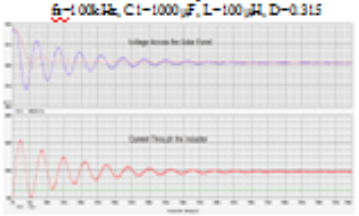

9.3. PCB Layout

Bottom Copper Layer

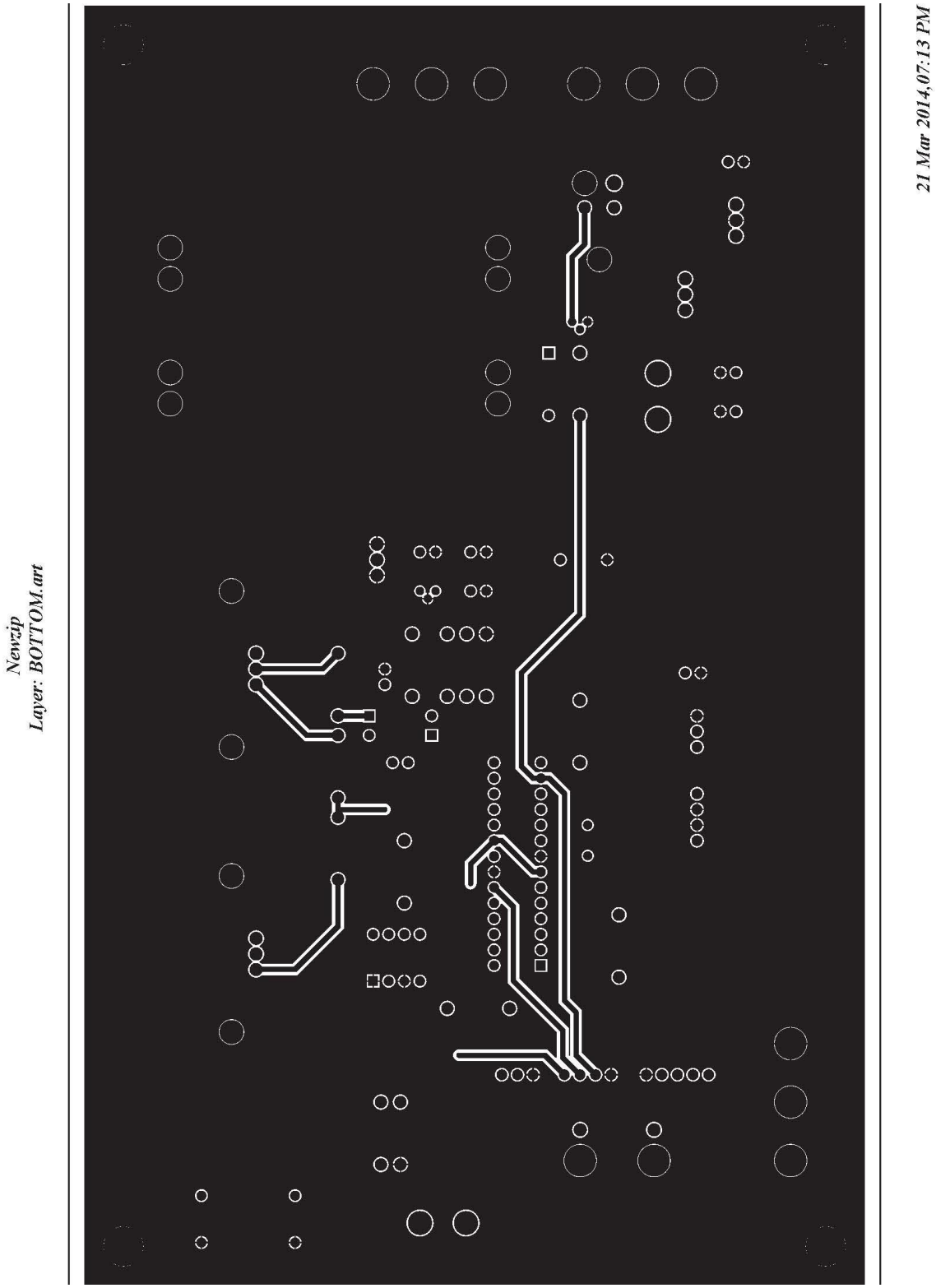

Top Silkscreen Layer

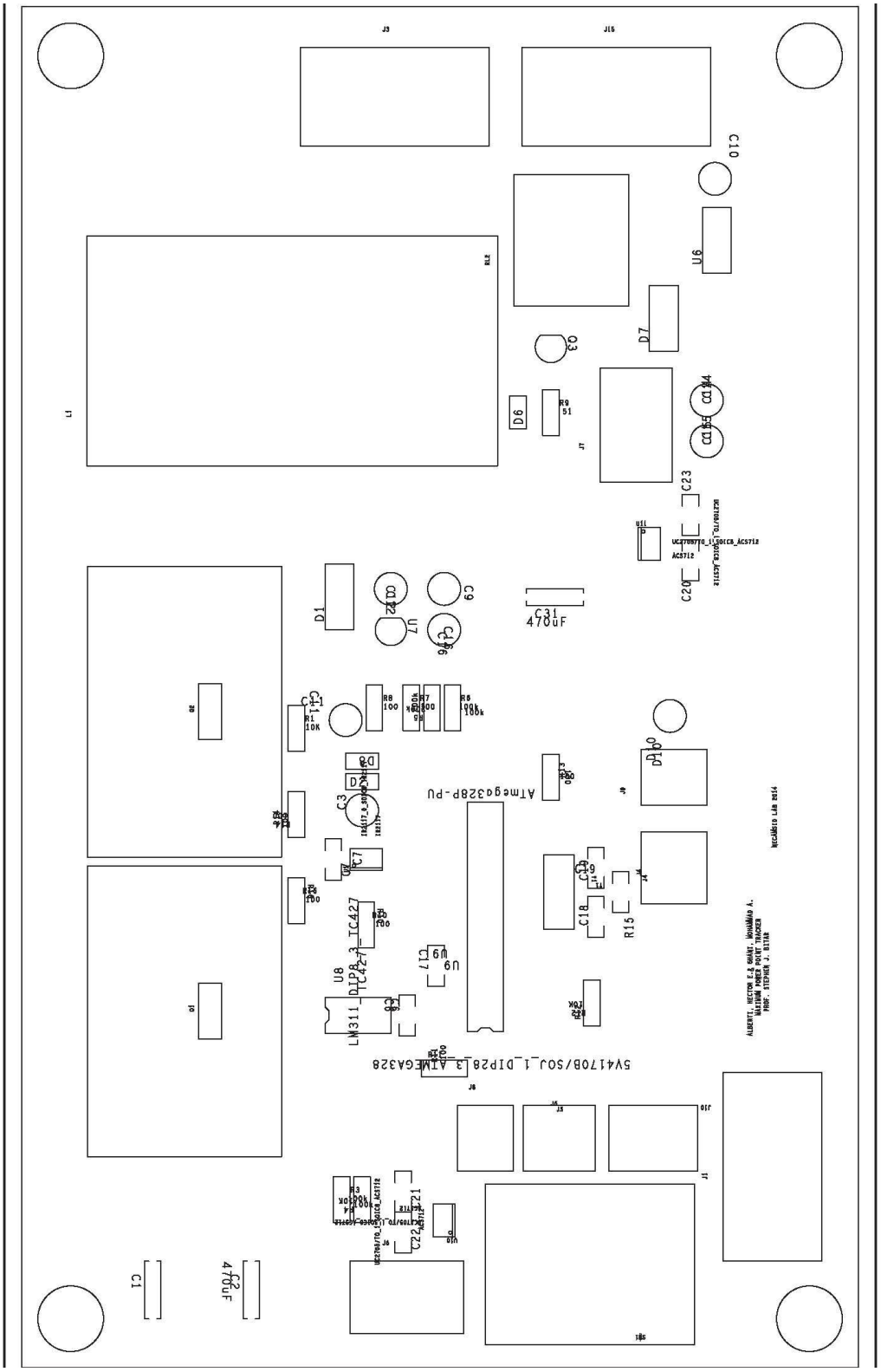

Top Copper Layer

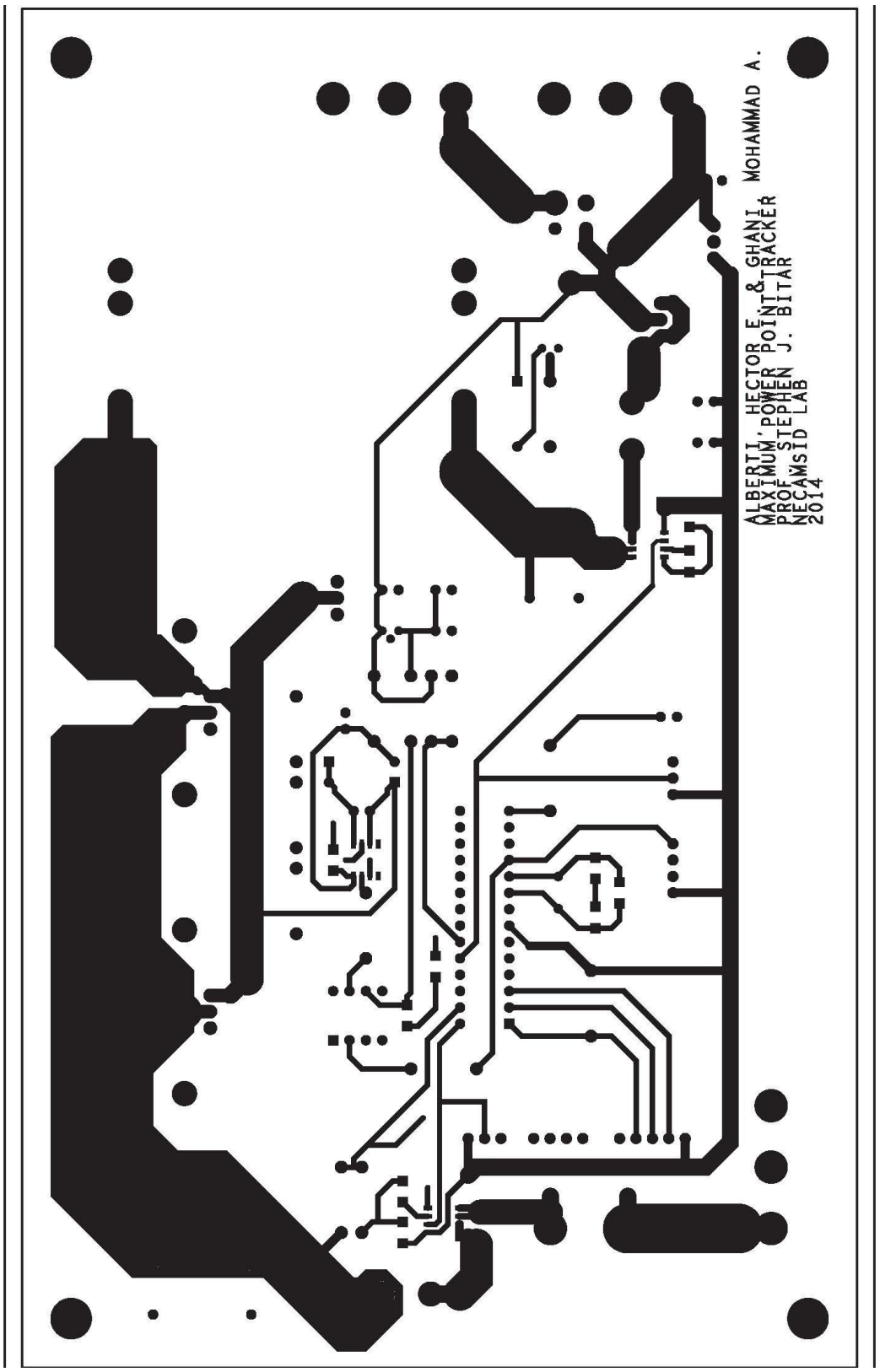

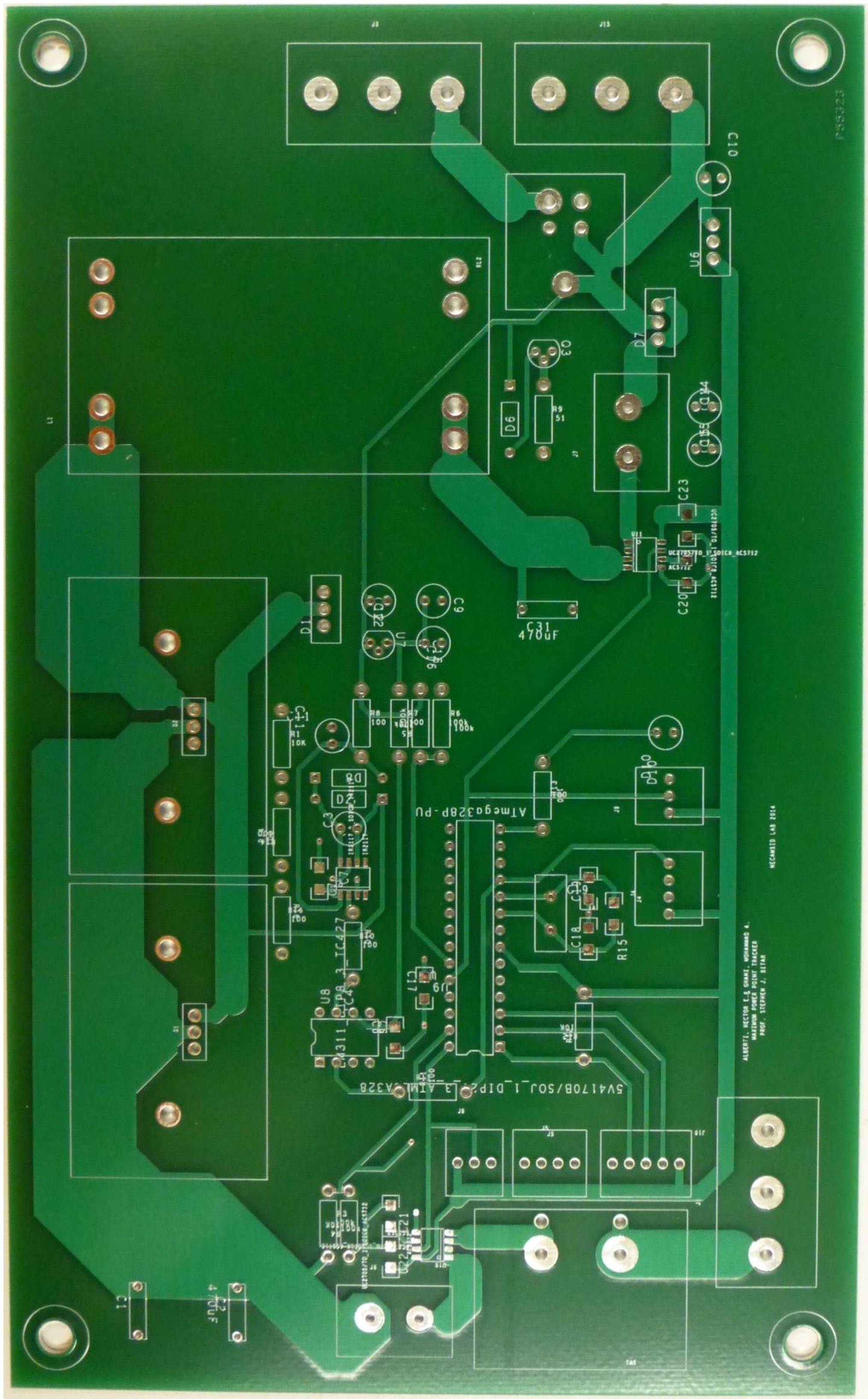
ATmega328P-PU
C31
470uF
C10
V6
D6
R9
51
C23
C20
C9
D1
Q3
D7
C18
R15
U8

9.4. Data from 03/16/2014 at 3:40 pm

Duty Cycle	V_in	I_in	P	V_out	I_out
1	48.47	-0.04	-1.9388	12.8	-0.16
2	48.47	-0.04	-1.9388	12.8	-0.16
3	48.4	0.01	0.484	12.78	-0.17
4	48.42	-0.01	-0.4842	12.79	-0.15
5	48.38	-0.02	-0.9676	12.79	-0.12
6	48.35	-0.01	-0.4835	12.78	-0.17
7	48.34	-0.04	-1.9336	12.73	-0.14
8	48.38	-0.02	-0.9676	12.77	-0.14
9	48.34	-0.04	-1.9336	12.73	-0.14
10	48.37	0	0	12.83	-0.16
11	48.38	-0.03	-1.4514	12.71	-0.16
12	48.38	0	0	12.78	-0.12
13	48.48	0.01	0.4848	12.75	-0.14
14	48.43	-0.03	-1.4529	12.86	-0.14
15	48.35	0	0	12.76	-0.1
16	48.38	0.02	0.9676	12.75	-0.15
17	48.39	-0.02	-0.9678	12.73	-0.12
18	48.52	-0.01	-0.4852	12.8	-0.09
19	48.34	0.03	1.4502	12.68	-0.11
20	48.33	0.05	2.4165	12.86	-0.08
21	48.54	-0.01	-0.4854	12.77	-0.04
22	48.18	0.02	0.9636	12.85	0.03
23	48.22	0.08	3.8576	12.97	0.16
24	48	0.27	12.96	12.91	0.86
25	47.54	0.6	28.524	12.86	1.99
26	46.85	1.01	47.3185	12.61	2.88
27	46.52	1.45	67.454	12.64	3.89
28	45.84	1.78	81.5952	12.62	5
29	45.24	2.15	97.266	12.05	5.66
30	44.66	2.48	110.7568	11.86	6.09
31	44.68	2.57	114.8276	11.99	6.24
32	44.45	2.66	118.237	12.47	6.51
33	43.48	2.79	121.3092	11.51	6.7
34	43.61	2.99	130.3939	11.88	7.8
35	43.04	3.12	134.2848	11.72	7.59
36	42.54	3.18	135.2772	13.53	9.49
37	42.69	3.36	143.4384	11.33	7.08
38	41.79	3.54	147.9366	11.44	6.96

39	41.47	3.71	153.8537	12.74	8.03
40	40.92	3.9	159.588	12.32	8.09
41	40.42	3.85	155.617	13.62	7.98
42	40.33	3.92	158.0936	13.56	8.43
43	39.56	4.09	161.8004	12.11	9.42
44	38.42	4.19	160.9798	13.04	9.06
45	37.46	4.29	160.7034	13.8	8.76
46	36.07	4.34	156.5438	12.29	9.91
47	34.78	4.38	152.3364	12.62	8.44
48	33.48	4.31	144.2988	13.22	7.91
49	31.57	4.43	139.8551	13.41	7.56
50	30.57	4.42	135.1194	13.22	7.37
51	30.04	4.36	130.9744	12.49	8.62
52	27.93	4.35	121.4955	13.11	7.62
53	27.3	4.38	119.574	13.75	7.58
54	26.63	4.36	116.1068	13.31	7.28
55	26.18	4.36	114.1448	13.49	7.19
56	25.61	4.31	110.3791	12.91	7.19
57	24.98	4.3	107.414	13.8	6.88
58	24.57	4.31	105.8967	13.48	6.84
59	24.26	4.26	103.3476	13.92	6.71
60	23.68	4.28	101.3504	13.66	6.5
61	23.31	4.27	99.5337	13.96	6.68
62	22.78	4.26	97.0428	13.48	6.45
63	22.37	4.29	95.9673	14.12	6.37
64	22.08	4.28	94.5024	13.99	6.13
65	21.74	4.26	92.6124	13.67	6.24
66	21.36	4.26	90.9936	14.04	6.16
67	20.95	4.31	90.2945	13.52	5.98
68	20.67	4.31	89.0877	14.17	5.93
69	20.33	4.31	87.6223	14.14	5.84
70	20.05	4.28	85.814	14.46	5.83
71	19.91	4.33	86.2103	13.67	5.75
72	19.43	4.33	84.1319	13.68	5.63
73	19.12	4.36	83.3632	14.18	5.49
74	18.67	4.33	80.8411	14.67	5.56
75	18.54	4.29	79.5366	14	5.41
76	18.29	4.28	78.2812	13.85	5.32
77	17.98	4.35	78.213	14.35	5.24
78	17.63	4.31	75.9853	14.19	5.21
79	17.68	4.34	76.7312	14.14	5.24

80	17.18	4.28	73.5304	14.35	5.16
81	16.98	4.32	73.3536	14.32	5.03
82	16.8	4.29	72.072	14.28	4.96
83	16.69	4.31	71.9339	14.54	4.91
84	16.35	4.33	70.7955	14.12	4.88
85	16.06	4.31	69.2186	14.15	4.79
86	16.03	4.26	68.2878	14.37	4.8
87	15.63	4.36	68.1468	14.33	4.7
88	15.7	4.29	67.353	14.33	4.71
89	15.41	4.33	66.7253	14.27	4.63
90	15.18	4.33	65.7294	14.17	4.56